Available online at www.sciencedirect.com
ScienceDirect
Coordination Chemistry Reviews 252 (2008) 212–230
COORDINATION CHEMISTRY REVIEWS
www.elsevier.com/locate/ccr

Review

# Aspects of dihydrogen coordination chemistry relevant to reactivity in aqueous solution

Nathaniel K. Szymczak, David R. Tyler*

*Department of Chemistry, 1253 University of Oregon, Eugene, OR 97405, United States*

Received 9 May 2007; accepted 12 June 2007
Available online 17 June 2007

## Contents



## Abstract

The aqueous coordination chemistry of dihydrogen has potential applications in inorganic biomimicry, chemoselective hydrogenation catalysis, and green chemistry. However, experimental and mechanistic studies that explore the aqueous behavior of these complexes are virtually unknown. This review identifies the motivation for studying aqueous dihydrogen coordination complexes by providing a summary of reactions that involve a dihydrogen ligand in highly polar solvents. The under-utilized potential of aqueous dihydrogen complexes in ionic hydrogenation reactions and in biomimicry is addressed. Finally, NMR methods for characterizing H–H bond distances in $\eta^2$-$H_2$ complexes are reviewed.


*Keywords:* Aqueous coordination chemistry; Dihydrogen complex; Hydrogen bonding; Hydrogenase; Proton transfer

* Corresponding author. Tel.: +1 541 346 4649; fax: +1 541 346 0487.
*E-mail address:* dtyler@uoregon.edu (D.R. Tyler).

0010-8545/$ – see front matter © 2007 Elsevier B.V. All rights reserved.
doi:10.1016/j.ccr.2007.06.007

## 1. Introduction

### 1.1. Overview

The seminal discovery by Kubas et al. [1] of an unusual class of compounds now known as σ-bonded complexes prompted a vast research effort to understand their structure, function and reactivity [2–6]. σ-Bonded dihydrogen complexes (i.e., $\eta^2$-$H_2$ complexes) in particular have been the subject of especially intense investigation because they have been shown to be key intermediates or precursors in a variety of catalytic transformations involving $H_2$ as a reactant [7,8]. While much is known about the non-aqueous reactivity of dihydrogen complexes, specifically with regard to catalysis, very few studies have identified, much less examined, water-soluble dihydrogen complexes and their solution behavior. Aqueous coordination chemistry has many desirable attributes. Of particular interest is the extension of known non-aqueous catalytic reactions into aqueous media to reduce the use of environmentally hazardous solvents and to increase atom economy. Also, because the dielectric constant of water is exceptionally high, water is a particularly desirable medium in which to perform reactions that feature a charged transition state. Furthermore, hydrogenation reactions that proceed through an ionic mechanism may selectively promote reactions at a polar group in the presence of non-polar functionalities. It has been suggested that the selectivity should be maximized when performed in an ionizing, polar solvent such as water [9–11].

Although heterolytic proton transfer reactions play a prominent role in many catalytic cycles, including the hydrogenase-mediated reduction of protons, there has been limited experimental success at identifying key intermediates in such reactions. Many of these intermediates are proposed to contain unique hydrogen-bonded species; however, their identity in solution has been unconfirmed up to now.

The focus of this review is information relevant to the chemistry of dihydrogen σ-complexes in aqueous solution. We begin with a brief background section on the bonding and structure in $\eta^2$-$H_2$ complexes, followed by a short discussion of known aqueous $\eta^2$-$H_2$ complexes, and then proceed to a general description of the non-aqueous reactivity of dihydrogen complexes in polar media. The heterolytic reactivity trends as they relate to ionic-type hydrogenation reactions will be discussed, followed by a brief survey of known ionic hydrogenation reactions that proceed through an $\eta^2$-$H_2$ precursor or intermediate. Such reactions are of particular interest because they are an initial step toward utilizing an ionic mechanism in hydrogenation reactions. A thorough understanding of the mechanism of these ionic hydrogenations, as well as a knowledge of the solution-phase properties of dihydrogen complexes in water, is required before effective catalytic cycles involving $H_2$ intermediates can be realized in water. Because of their relevance to heterolytic $H_2$ activation, intermediates in proton transfer reactions will also be discussed, specifically with regard to hydrogen bonded species, including a novel dihydrogen hydrogen bonding motif. Finally, NMR characterization methods of $\eta^2$-$H_2$ complexes will be reviewed.

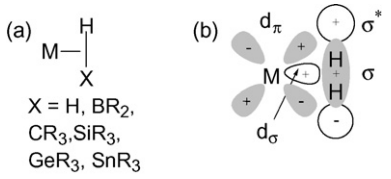


Fig. 1. The coordination of a generic HX σ bond (a) to a transition metal center, and (b) a pictorial description of the bonding in σ-complexes with $H_2$ as a prototype. Filled orbitals are shaded gray, empty orbitals are unshaded.

### 1.2. Bonding and structure of $\eta^2$-$H_2$ complexes

The bonding in $\eta^2$-$H_2$ complexes and σ complexes, in general, is described by the Dewar–Chatt–Duncanson bonding model [12], which entails electron donation from the σ bond of the ligand to an empty metal orbital accompanied by back-donation from a filled d-orbital into the σ* orbital of the ligand (Fig. 1).

The backbonding is a crucial component of this bonding, much as it is in the bonding of olefins and CO to a transition metal fragment. Just as the $\nu$(C≡O) in an infrared spectrum gives electronic information on the extent of π-back-bonding, the H–H bond distance ($d_{HH}$) gives analogous information for a coordinated $H_2$ ligand. Accordingly, the extent that the H–H bond is elongated from the distance in the free molecule (0.74 Å) is a typical characterization criterion for $H_2$ σ-complexes. In this regard, one can consider a σ-bonded $H_2$ complex as an arrested intermediate along the oxidative-addition pathway. Indeed, H–H bond distances have been measured in complexes that span the spectrum from free $H_2$ to classical dihydrides (Fig. 2).

Coordination of $H_2$ to a transition metal center results in several changes in the properties of the $H_2$ molecule, and activation (both homolytic and heterolytic) is usually facile. The electronic features of the transition metal fragment determine which activation pathway is followed, and heterolytic activation of $H_2$ is typically favored for highly electrophilic fragments or complexes containing highly π-acidic *trans* ligands. While the acidity of free $H_2$ is negligible in THF ($pK_a > 49$) [13], the $pK_a$ can drop substantially upon coordination to a transition metal. Indeed, one potential way of utilizing $\eta^2$-$H_2$ coordination complexes in water is to deliver acid equivalents generated from $H_2$ gas to a substrate. For instance, when $H_2$ gas coordinates to a highly electrophilic rhenium fragment to form $[Cp^*Re(H_2)(CO)(NO)]^+$, it becomes superacidic ($pK_a = -2$ in $CH_2Cl_2$) [14]. In another example, the dicationic *trans*-$[Os(DPPE)_2(CO)(H_2)]^{2+}$ complex, prepared by protonation of the corresponding osmium hydride, has a reported $pK_a$ value close to −6 (pseudo-aqueous scale) [15]. Although such acidity

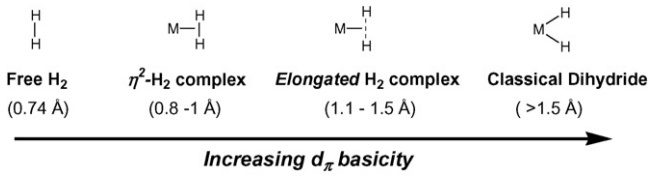


Fig. 2. The change in the H–H bond distance upon coordination to metal centers of increasing basicity.

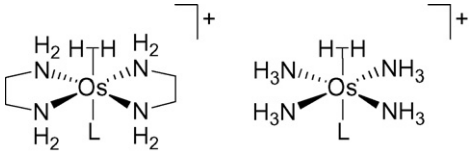

Fig. 3. The first reported water-soluble $\eta^2$-$H_2$ complexes.

represents an extreme case of binding to a super electrophilic metal fragment, more common p$K_a$ values of coordinated $H_2$ range between 5 and 16 p$K_a$ units [5,13,16–18]. A consequence of the increased acidity of coordinated $H_2$ is the propensity for deprotonation by a suitable base. Thus, although the H–H bond in free dihydrogen is quite strong (104 kcal mol$^{-1}$), the heterolytic activation of $H_2$ is a common reaction pathway that allows an $H_2$ molecule to be effectively cleaved into $H^+$ and $H^-$ [5,19,20]. The proton transfer heterolytic activation pathway (Eq. (1)) can proceed intermolecularly to an external base or intramolecularly to a nearby ligand. This type of reactivity is crucial to many biological and industrial systems that utilize $H_2$ as a feedstock [21].

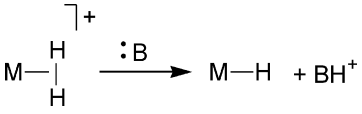

(1)

## 2. Water-soluble $\eta^2$-$H_2$ complexes

As discussed in the sections below, water-soluble, inert $\eta^2$-$H_2$ complexes show potential for use in a wide variety of applications, ranging from biomimicry to selective hydrogenation catalysis. Yet, until relatively recently, few such complexes were known. The first *water-soluble* dihydrogen complexes were reported by Malin and Taube [22], although the complexes were not recognized as $\eta^2$-$H_2$ complexes until some 20 years later [23]. Taube synthesized the $[Os(NH_3)_4(H_2)(L)]^+$ complex and the corresponding ethylene diamine (en) species (Fig. 3) in water by the routes in Eqs. (2) and (3). Subsequent analyses by diffraction [24,25] and NMR spectroscopy [26] showed that both complexes have *elongated* $\eta^2$-$H_2$ ligands. It needs to be stressed that using water in these syntheses was not (and is not) typical of the methods used to prepare $\eta^2$-$H_2$ complexes. Most coordination complexes of dihydrogen are generated in non-polar and, typically, non-coordinating solvents.

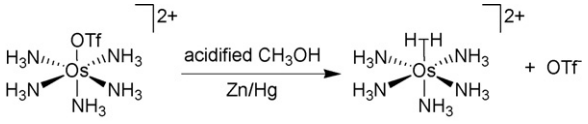

(2)

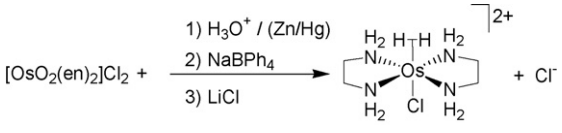

(3)

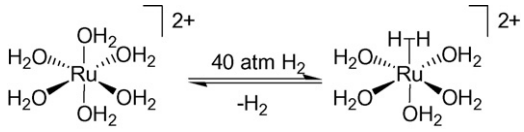

Fig. 4. The $[Ru(H_2O)_5(H_2)]^{2+}$ complex was generated *in situ* under a high pressure of $H_2$.

The complexes synthesized by Taube are unexpectedly robust with regard to loss of $H_2$ in aqueous solutions or solutions containing highly coordinating solvents such as pyridine and acetonitrile. However, the ligand *trans* to the $\eta^2$-$H_2$ ligand was easily displaced by a variety of neutral and anionic ligands, including water. As a practical application, it was found that *trans*-$[Os(en)_2(H_2)(L)][PF_6]$ binds to a variety of biomolecules, including nucleotides, RNA, amino acids, peptides, and phospholipids. The chemical shift of the $H_2$ resonance was a sensitive probe of the *trans* ligand [27], and the ease of substitution of the *trans* ligand and its subsequent effect on the $^1$H NMR spectrum of the $\eta^2$-$H_2$ ligand was exploited for molecular recognition.

Another water-soluble, yet unstable, $\eta^2$-$H_2$ complex was generated *in situ* by charging a solution of $[Ru(H_2O)_6]^{2+}$ with 40 atm of $H_2$ (Fig. 4) [28]. This complex is unusual in several respects. The coordination sphere around the ruthenium does not contain any π-acidic or π-basic ligands, which is quite atypical of most ligand architectures that support an intact dihydrogen ligand. The solution structure of the complex was confirmed by $^{17}$O NMR spectroscopy at 533 atm $H_2$, and the identity of the coordinated $H_2$ ligand was shown by a large $J_{HD}$ and small $T_1$ value of the $H_2$ resonance (see Section 5). This complex was also found to catalyze H/D exchange with the $D_2O$ solvent and $H_2$, and at the high pressures used, HD gas was observed spectroscopically.

Recently, another class of water-soluble and stable $\eta^2$-$H_2$ complexes was reported from our laboratory [29,30]. When a water-soluble iron bis(phosphine) complex was charged with a low pressure of $H_2$ (1–2 atm) in water, the corresponding dihydrogen hydride species formed (Fig. 5).

The formation of the dihydrogen complex was investigated by variable temperature multinuclear NMR experiments and shown to follow a pathway involving phosphine-assisted heterolytic cleavage of $H_2$. (Note the formation of the protonated phosphine in Fig. 5.) Once the phosphine was protonated, it underwent decoordinative decomposition and scavenged some of the acid produced. Control experiments showed that the pH of the ending solution corresponded with the p$K_a$ values of the protonated phosphine ligands. To circumvent the decomposition

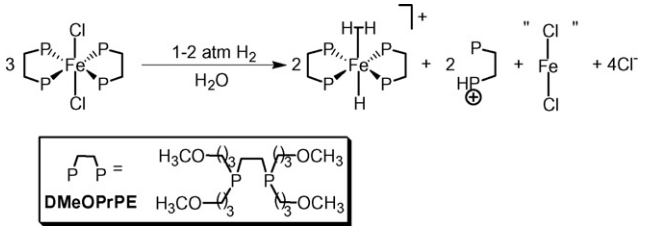

Fig. 5. The $[Fe(DMeOPrPE)_2(H)(H_2)]^+$ complex is generated at near atmospheric pressure of $H_2$ along with acid-promoted decomposition products.

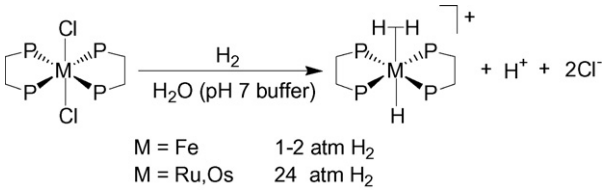


Fig. 6. The $[M(DMeOPrPE)_2(H)(H_2)]^+$ complexes (M = Fe, Ru, Os) are generated quantitatively when reacted in buffered solutions.

pathway, the dihydrogen complex could be formed quantitatively when reacted in a buffered solution (pH 7). The analogous ruthenium [31] and osmium species [32] were also found to yield a water-soluble and stable dihydrogen hydride complex in buffered solution at slightly higher pressures of $H_2$ (*ca.* 24 atm) (Fig. 6).

Although the above examples represent the known $\eta^2$-$H_2$ coordination complexes in water, numerous other reports have proposed intermediates consisting of $\eta^2$-$H_2$ complexes in water, particularly to explain H/D exchange in $D_2O$ as well as potential intermediates in hydrogenase enzymes [33–40]. These examples are discussed in the sections below where appropriate.

## 3. Reactivity of $H_2$ complexes

### 3.1. General non-aqueous reactivity

When an $\eta^2$-$H_2$ complex is involved in a catalytic or stoichiometric reaction, the $\eta^2$-$H_2$ ligand does one of the following: (1) it readily dissociates to provide an open coordination site; (2) it acts as a proton or hydride donor to an appropriate substrate, or (3) it provides reducing equivalents to a metal center for later use. These reactions are outlined in Scheme 1 for both homolytic and heterolytic cleavage pathways. The homolytic pathway is typically favored for highly basic transition metal centers, while the heterolytic pathway is favored for electrophilic metal complexes. Because most catalytic processes involving $H_2$ employ

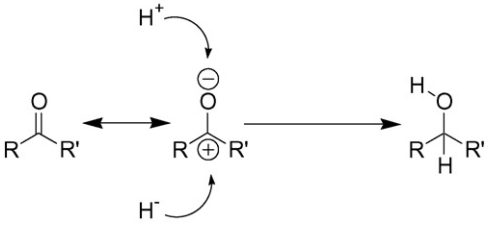


Scheme 2. A general schematic representation for the ionic hydrogenation of a polar double bond.

highly basic transition metal centers, the homolytic pathway is most typical. The catalytic chemistry of $H_2$ through homolytic activation pathways has been extensively reviewed [5,7,8,41]. In contrast, catalytic reactions proceeding through heterolytic routes are less studied [7,21].

### 3.2. Heterolytic reactivity of $\eta^2$-$H_2$ complexes: stoichiometric ionic hydrogenation reactions

The heterolytic cleavage of $H_2$ is proposed to be an important step in reactions involving H/D exchange [42] and various catalytic ionic hydrogenations and hydrogenolysis reactions [21,43]. An *ionic* hydrogenation involves the sequential addition of $H^+$ and $H^-$ across a polar double bond (Scheme 2) [44]. Originally, this was achieved through the use of different external hydride or proton sources, but such reactions have the potential to utilize both fragments from the heterolytic cleavage reaction of $H_2$.

Kursanov et al. provided an early example of ionic hydrogenation reactions by using separate acid and hydride sources [45]. A variety of olefins and ketones were stoichiometrically hydrogenated using $Et_3SiH$ as a hydride source and $CF_3COOH$ as a proton source. It was later recognized that the source of a hydride need not be a typical organic hydride source such as a silane. Reports by Darensbourg and co-workers [46] and Gibson and El-Omrani [47] showed that certain early metal hydride

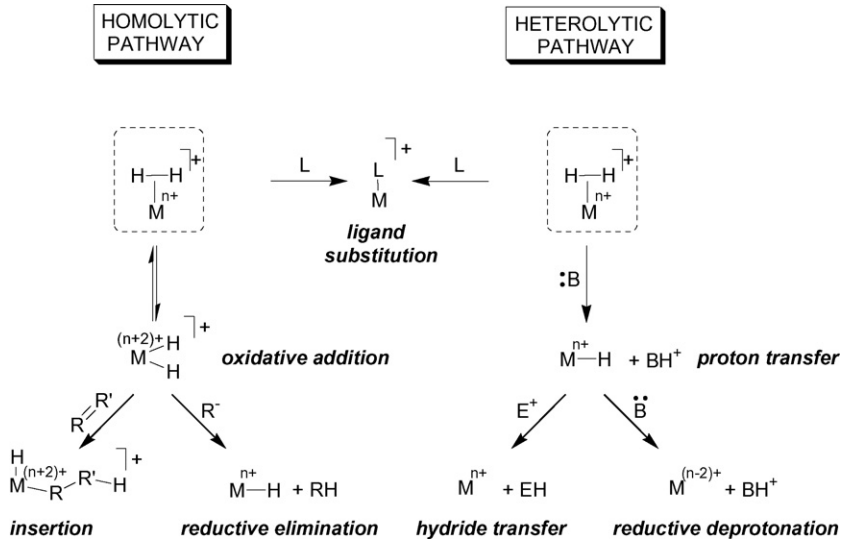


Scheme 1. Homolytic and heterolytic reaction pathways for $\eta^2$-$H_2$ complexes. B represents a generic base, E represents an electrophile.

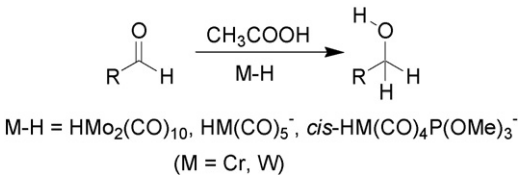


Fig. 7. Ionic hydrogenation of an aldehyde using group 6 hydrides.

complexes are sufficiently hydridic to hydrogenate aldehydes through an ionic mechanism (Fig. 7).

Bullock later showed that ionic hydrogenations of less reactive substrates were possible, and using $WCp(CO)_3H$ and triflic acid he was able to effect the hydrogenation of ketones and substituted olefins [48]. In the case of ketone hydrogenation, unexpectedly, the *kinetic* product of hydrogenation was isolated as an alcohol-coordinated species, stabilized by a hydrogen bond to the triflate anion (Fig. 8) [49].

It was subsequently found that the hydrogen-bonded adduct retained its structure in solution as well as in the solid state. Additionally, the hydrogen-bonded adducts were general to a variety of ketones and aldehydes including 2-adamantanone, cyclohexanone, and propionaldehyde. Hydrogen-bonding interactions are presumed to facilitate the proton transfer event.

### 3.3. Catalytic ionic hydrogenations involving $\eta^2$-$H_2$ complexes

Because metal hydrides and protons can be generated directly by heterolytic cleavage of $H_2$ on a transition metal center, the scope of ionic hydrogenations has been extended to catalytic systems in which $H_2$ acts as both the proton and hydride source. In this regard, dihydrogen complexes are ideal catalysts because $\eta^2$-$H_2$ complexes typically have a high kinetic acidity [4,5], and the resulting hydride can be substantially hydridic [44].

A general mechanistic scheme for an ionic hydrogenation involving an $\eta^2$-$H_2$ complex is shown in Scheme 3. Because of the charged and polar species involved in this pathway, ionic-hydrogenation reactions lend themselves to ionizing solvents such as alcohols and water [9]. For this reason, the ionic hydrogenation pathway shows promise for selectively hydrogenating polar C=O and C=N bonds in the presence of C–C olefinic and acetylenic bonds [10,11]. It is also noted that reactions of $H_2$

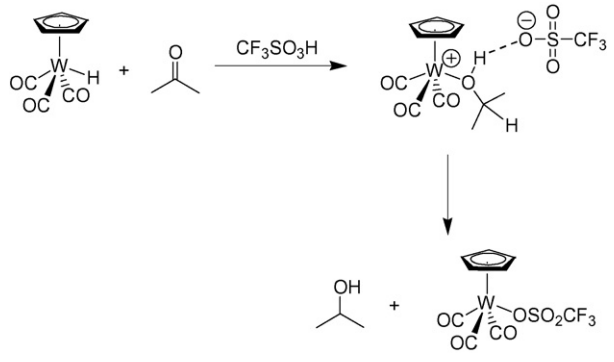


Fig. 8. A stoichiometric ionic hydrogenation of acetone using $WCp(CO)_3H$ as a hydride source.

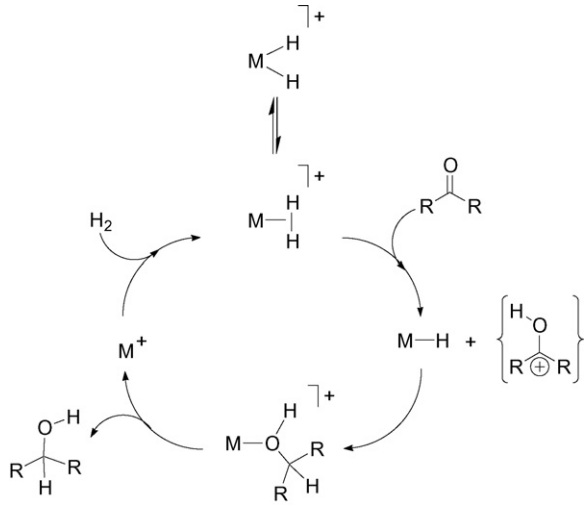


Scheme 3. Proposed mechanism for catalytic ionic hydrogenations of ketones by an $\eta^2$-$H_2$ complex.

in biological systems proceed through heterolytic routes where $H^+$ and $H^-$ are transferred separately to a substrate. In this sense, ionic hydrogenations involving $\eta^2$-$H_2$ complexes mimic biological reductions.

Several complexes have been shown to be viable catalysts for hydrogenation reactions proceeding through an ionic pathway. Ideally, the kinetic acidity of the $H_2$ complex should be reasonably high so that it can act as a proton donor to the substrate and concomitantly regenerate the metal hydride. Conversely, the resultant hydride should be sufficiently hydridic to affect a hydride transfer to an electrophilic substrate.

Several $\eta^2$-$H_2$ or dihydride complexes show promise as ionic hydrogenation catalysts (Fig. 9). For instance, ruthenium complexes bearing either Cp or Cp* and carbonyl ligands or bidentate phosphine chelates provide access to the necessary ionic hydrogenation prerequisites. The complex $[Ru(Cp^*)(CO)_2(H_2)]^+$ is so acidic that it is deprotonated by diethyl ether [14], while the $pK_a$ values of the coordinated $\eta^2$-$H_2$ ligand in complexes of the type $Ru(Cp)(P_2)(H_2)^+$ are typically between 7 and 9 (measured in THF or $CH_2Cl_2$) and are also readily deprotonated [50,51]. Bullock has determined the hydricity of the several resultant hydride species by comparing the rate constants of hydride transfer to the trityl cation ($Ph_3C^+$) measured using stopped-flow techniques [52,53]. The $Ru(Cp^*)(CO)_2(H)$ complex delivers its hydride equivalent at an impressive rate (estimated $k_{H^-} \approx 5 \times 10^6\ M^{-1}\ s^{-1}$), which is illustrative of its potential as a potent hydride donor.

#### 3.3.1. Molybdenum and tungsten hydrides for ionic hydrogenations

Molybdenum and tungsten Cp complexes containing carbonyl and phosphine ligands are active ionic hydrogenation catalysts. The hydricity of these species is diverse and very sensitive to the identity of ancillary ligands (Table 1). Additionally, the acidity of the cationic molybdenum and tungsten dihydride species is considerable, as protonation of $CpW(CO)_3H$ with a strong acid resulted in only 16% of the corresponding dihy-

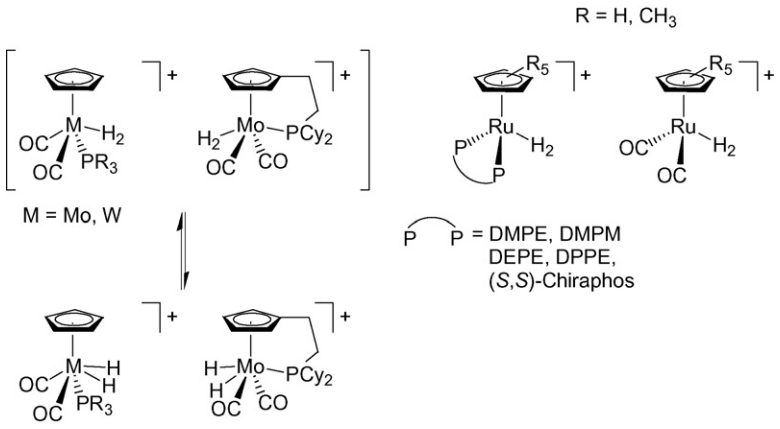


Fig. 9. Several examples of proposed active catalysts used by Bullock and Norton for catalytic ionic hydrogenation reactions. Note that in the case of Mo or W species, an intermediate $\eta^2$-$H_2$ species may only be formed transiently and the dihydride tautomer results.

Table 1
Rate constants for hydride transfer from metal hydrides to $[Ph_3C][BF_4]$ ($CH_2Cl_2$, 25 °C)

| Metal hydride | $k_{H^-}$ ($M^{-1}$ $s^{-1}$) |
|---|---|
| $CpW(CO)_3H$[a] | $7.6 \times 10^1$ |
| $HSiEt_3$[a] | $1.5 \times 10^2$ |
| $CpMo(CO)_3H$[a] | $3.8 \times 10^2$ |
| $CpMo(CO)_2(PCy_3)H$[a,b] | $4.3 \times 10^5$ |
| $CpMo(CO)_2(PPh_3)H$[a,b] | $5.7 \times 10^5$ |
| $CpMo(CO)_2(PMe_3)H$[a,b] | $4.6 \times 10^6$ |
| $Cp^*Ru(CO)_2(H)$[c] | $\approx 5 \times 10^6$ |

[a] Ref. [53].
[b] $PCy_3$ = tricyclohexyl phosphine, $PMe_3$ = trimethyl phosphine, $PPh_3$ = triphenyl phosphine.
[c] Ref. [52].

dride, implying that the dihydride is a stronger acid than HOTf [54].

A study of the protonation of $CpW(PMe_3)(CO)_2H$ showed that the kinetic site of protonation is the W–H bond, suggesting an intermediate $W(H_2)^+$ species [55]. The existence of an $\eta^2$-$H_2$ complex may only be transient, however, as the dihydride version dominates in solution [54]. Regardless of the tautomeric form of the dihydride species, the rates of hydrogenation were found to be slow. Also, the Mo and W catalysts suffered decomposition from a competitive phosphine protonation/decoordination pathway. To prevent decomposition and enhance catalytic rates in the Mo-system, an appended phosphine was installed on a cyclopentadienyl ring to inhibit phosphine dissociation [56]. Unfortunately, this modification afforded even *slower* rates (3× slower), although it did substantially increase the thermal stability and lead to longer catalyst lifetimes of several hundred turnovers. Clearly, further improvements are required for group 6 metal hydride systems before their utility is realized.

### 3.3.2. *RuCp(P$_2$)H systems for ionic hydrogenations*

The ruthenium piano-stool complexes were shown by Norton and co-workers to be viable catalysts for the hydrogenation of imines, iminium ions, ketones, and aziridines [57,58]. In order to optimize the catalysts for selective hydrogenation reactions, several parameters of the complex were adjusted. The size of the phosphine chelate was varied to examine how it affected the rate of hydride transfer to an iminium cation. It was found that the smaller the chelate ring size, the faster the hydride transfer, giving the following trend in the rates: CpRu(DPPM)H > CpRu(DPPE)H ≈ CpRu(DPPBz)H > CpRu(DPPP)H ≫ CpRu(DPPB)H [59]. This trend was rationalized by considering the effect that the ring size has on the energy of the LUMO. The energy of the unsaturated $CpRu(P_2)^+$ cation decreases as the chelate ring becomes larger, making the hydride more stable, and consequently less able to transfer away from the $CpRu(P_2)H$ fragment. Accordingly, the best catalyst for the selective hydrogenation of iminium ions was found to contain the DPPM phosphine.

Further studies aimed at determining selectivity and inhibition conditions found that when the iminium ion was located within the same molecule as a terminal olefin, hydrogenation was not catalytic. Presumably, this was due to competitive coordination of the olefin with $H_2$. In support of this hypothesis, when the olefin contained sterically blocking substituents to prevent it from competitively coordinating with $H_2$, selectivity of the C=N double bond was achieved over the C=C double bond (Eq. (4)) [57].

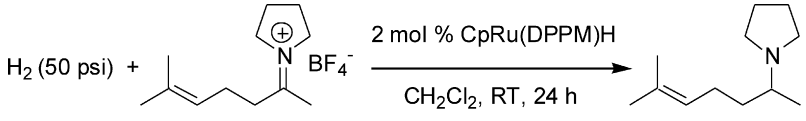


(4)

The $CpRu(P_2)H$ system can be tuned for asymmetric catalysis. For example, when a chiral diphosphine ligand such as (*S*,*S*)-Chiraphos was used, the resulting amine product formed

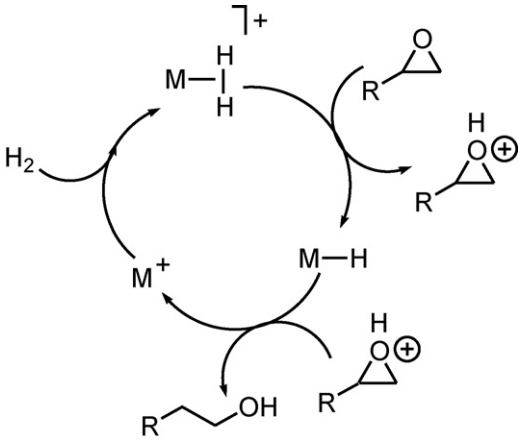

Scheme 4. Proposed mechanism for the catalytic ionic hydrogenation of epoxides using an $\eta^2$-$H_2$ complex to give the corresponding alcohols.

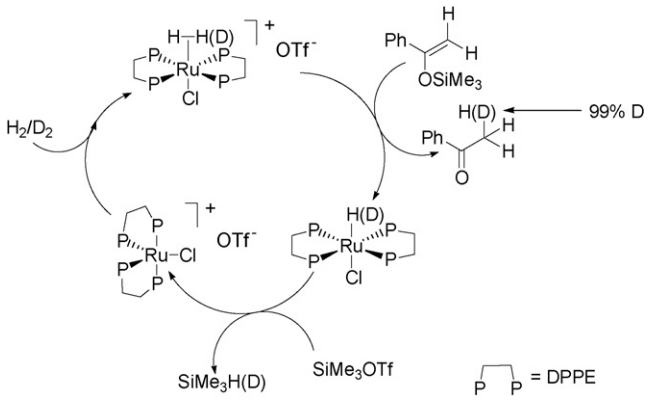

Scheme 5. A proposed mechanism for the catalytic hydrogenolysis of trimethylsilyl enol ethers with the specific example shown for the conversion of α-trimethylsiloxystyrene to acetophenone.

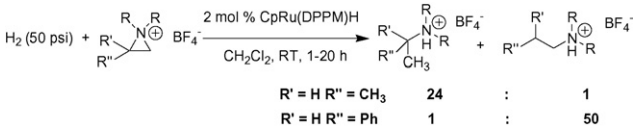

Fig. 10. The catalytic ionic hydrogenation of aziridinium ions by RuCp(DPPM)H gives regioselectivity based on the substituents at the 2-postion of the aziridinium cation.

with modest enantioselectively (Eq. (5)) [60].

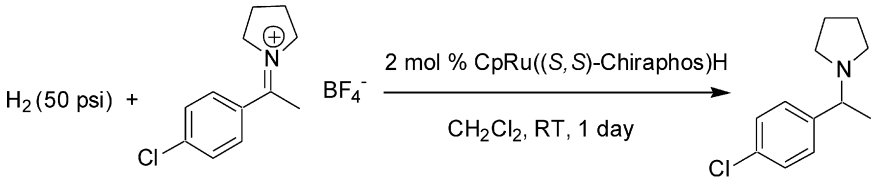

56 % ee (5)

The reactions above demonstrate the viability of using an ionic hydrogenation strategy to sequentially transfer protons and hydrides to an appropriate substrate. This method was extended to the goal of obtaining terminal alcohols catalytically by hydrogenation of epoxides (Scheme 4) [58].

A limitation to the investigations of such epoxide hydrogenations is the instability of the transiently formed protonated epoxide. This fact precluded a study of the mechanism of these reactions. To circumvent this problem, aziridinium ions were investigated. Aziridinium ions are isoelectronic to protonated epoxides but they have a higher thermal stability and are thus suitable models for studying the regiochemistry of hydride transfer to a protonated epoxide. In a recent study, Norton and coworkers found that the regiochemistry was controlled by the electronic properties of the R′ or R′ substituents (Fig. 10) [58]. Alkyl-substituted aziridinium cations gave the more branched ammonium cations, while the aryl-substituted aziridinium cation gave the less branched ammonium cations. This was rationalized by considering inductive effects on the acidity of the carbon at the 2-position. The electron-donating alkyl groups increase the electron density of the carbon at the 2-position and cause the carbon at the 1-position to be more susceptible to hydridic attack. Conversely, the electron-withdrawing phenyl group leads to a more acidic carbon, so it is more easily attacked by a hydride.

### 3.3.3. Hydrogenolysis of silyl enol ethers

Hidai showed that the acidity of a dihydrogen complex could be harnessed catalytically when coupled with a hydride-abstracting fragment such as a trialkyl silyl cation [61]. A specific example is shown in Scheme 5 where *trans*-$[Ru(DPPE)_2(H_2)Cl][OTf]$ and $SiMe_3OTf$ are used to effect a clean conversion of a silyl enol ether to a ketone and $Me_3SiH$. The mechanism in Scheme 5 was elucidated by deuterium labeling studies as well as by monitoring the stoichiometric reaction by $^1H$ NMR spectroscopy and was found to occur *via* heterolytic $H_2$ cleavage instead of an alternative dehydrosilylation mechanism. (The latter mechanism is the reverse reaction of the transition-metal-induced 1,4-addition of hydrosilanes to α,β-unsaturated carbonyl compounds [62,63].) Note that this mechanism is different from the previously discussed ionic hydrogenation pathways in that the proton and hydride are transferred to two separate molecules. Also noteworthy is the ease of deuteration at the α-position. Consequently, this type of reaction is a highly efficient means (85%+) for deuterium incorporation using $D_2$ gas as the sole source of deuterium.

The DPPE ligand in Scheme 5 was exchanged for a chiral bidentate phosphine ligand such as BINAP for the purpose of asymmetric hydrogenolysis of silyl enol ethers. Unfortu-

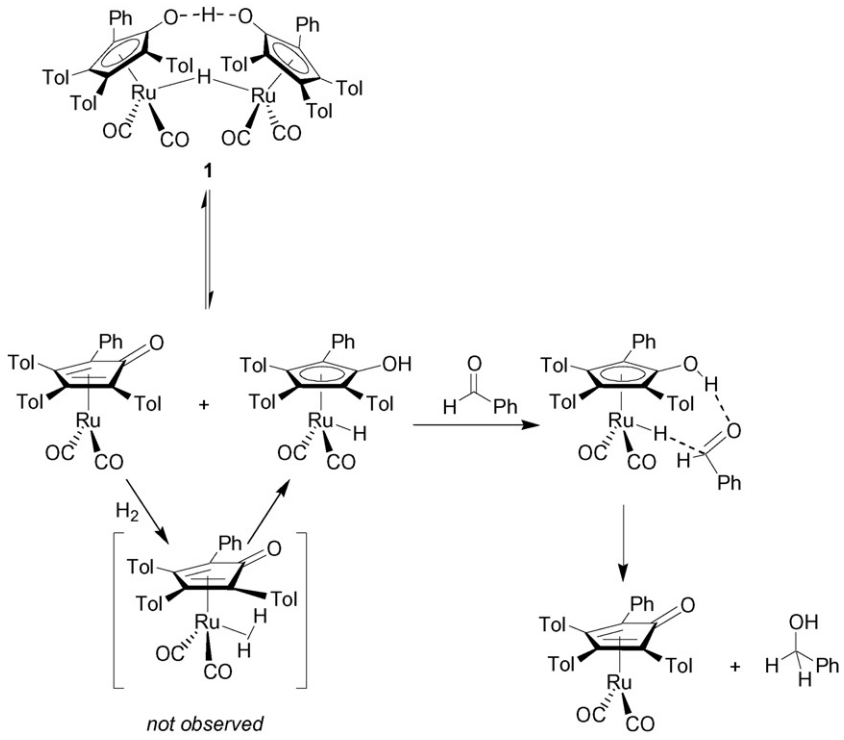


Scheme 6. Shvo's ruthenium catalyst hydrogenates polar double bonds by an outer-sphere ionic type mechanism. The dihydrogen species was not observed but is proposed as a logical intermediate to explain the reactivity.

nately, when the *trans*-[Ru(BINAP)$_2$(H$_2$)Cl][OTf] complex was reacted with $H_2$ gas and a prochiral trimethylsilyl enol ether, no enantioselectivity of the product alcohol was observed. This result indicated that the site of protonation is the oxygen atom of the silyl enol ether and *not* the sp$^2$ carbon. However, when the chiral BINAP catalyst was used in enolate systems, it was found that the system achieved enantioselective protonation of prochiral enolates in up to 75% *ee*, albeit not catalytically (Eq. (6)). Overall, this route provided a new approach using $H_2$ to effect the asymmetric protonation of enol ethers [61].

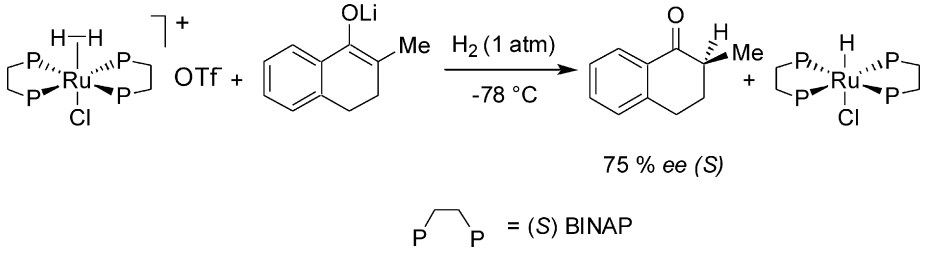


(6)

### 3.3.4. Shvo's system

The aryl-substituted cyclopentadienyl ruthenium system originally reported by Shvo et al. [64] (molecule **1** in Scheme 6) was shown to act as a catalyst for the hydrogenation of ketones, olefins, and acetylenes [65]. Mechanistic work by Casey et al. later showed that complex **1** catalyzes the hydrogenation of benzaldehyde by an outer-sphere ionic mechanism [66].

The acidity of the hydroxyl proton in Scheme 6 was confirmed to be high (3 p$K_a$ units more acidic than benzoic acid) and satisfies one of the prerequisites for an ionic mechanism, *vide supra*. Furthermore, deuterium isotope effects were investigated by selective deuteration of the hydroxyl and hydride positions. The observation of primary deuterium isotope effects for both Ru–D and O–D supported a concerted mechanism of hydrogen transfer in which Ru–H and O–D bond breaking occurs in the transition state. In addition, a second-order rate law was obtained (first-order each in aldehyde and Ru–H) as well as $\Delta S^{\ddagger} = -28$ eu, implying a concerted associative mechanism in which the hydride and proton are simultaneously transferred to the substrate. Although an $\eta^2$-$H_2$ complex was not directly observed in this system, its presence as an intermediate is almost certain. The proposed intermediate $H_2$ complex is similar to one reported by Heinekey, which was so acidic that diethyl ether acted as a base to deprotonate the coordinated $H_2$ [14]. In light of this result, it is reasonable to propose that the cyclopentadienone ligand in Scheme 6 can act as a base to deprotonate the initially formed $\eta^2$-$H_2$ complex at rate that exceeds the detection limits of $^1$H NMR spectroscopy.

An iron complex similar to the Shvo-type system was recently described by Casey and Guan [67]. This finding is noteworthy

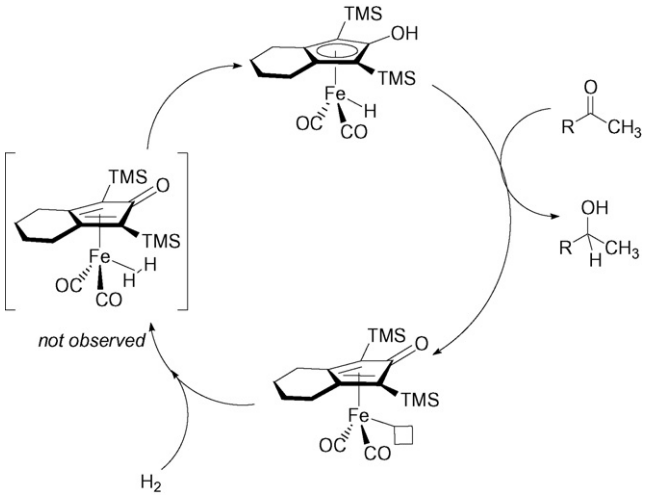


Scheme 7. A generalized catalytic scheme for the ionic hydrogenation of ketones using an iron hydride complex. The dihydrogen species was not observed, but, as in the Shvo mechanism in Scheme 6, is proposed here as a logical intermediate to explain the reactivity.

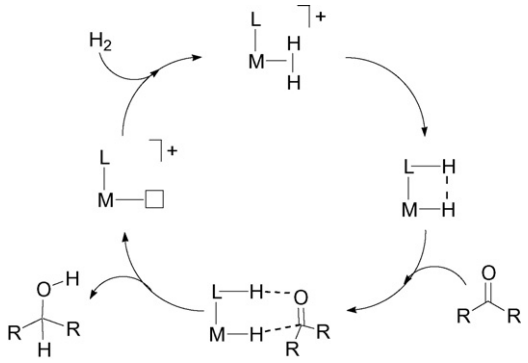


Scheme 8. A generalized scheme showing ionic hydrogenation of polar double bonds proceeding through an outer-sphere mechanism.

because it represents the first, well-defined iron catalyst for the hydrogenation of ketones, aldehydes and imines. The iron catalyst shows high functional group tolerance for carbon–halogen groups, nitro groups, and impressively even pyridine. The hydrogenation system also shows high chemoselectivity, as polar double bonds were selectively hydrogenated in the presence of olefinic or acetylenic groups (Scheme 7).

The second-order rate constant for the hydrogenation of acetophenone at 25 °C was $k = 9.8 \times 10^{-3}\ M^{-1}\ s^{-1}$. An Eyring plot yielded $\Delta H^{\ddagger} = 9.0 \pm 0.6$ kcal mol$^{-1}$ and $\Delta S^{\ddagger} = -37.5 \pm 2.1$ eu. Similar to Shvo's system, the large negative entropy of activation is consistent with a highly ordered transition state in which the ketone is strongly associated with the iron complex. Although not observed, a transient $\eta^2$-$H_2$ intermediate is likely heterolytically cleaved intermolecularly by the nearby ketone and utilized as a proton and hydride source. This work shows that, by exploiting the high kinetic acidity of a coordinated dihydrogen ligand, chemoselective hydrogenation reactions utilizing first-row metals are possible. Numerous substrates were selectively hydrogenated under remarkably mild conditions. Fig. 11 is presented to highlight the chemoselectivity, the lack of inhibition in the presence of competing ligands, and the mild conditions used in these reactions.

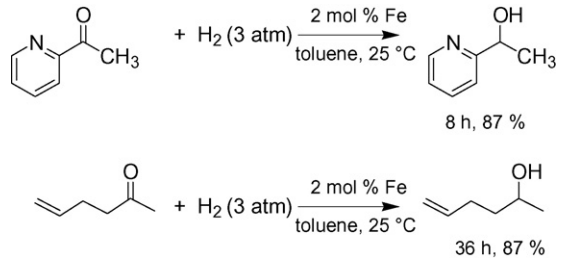


Fig. 11. Selected examples of chemoselective ionic hydrogenation using an iron catalyst.

### 3.3.5. *Noyori-type hydrogenation systems*

Hydrogenation catalysts based on Noyori's chiral diphosphine/diamine-$RuCl_2$ complexes have seen extensive use for the enantioselective hydrogenations of polar double bonds [11,68]. Noteworthy is the selectivity for the hydrogenation of polar C=N and C=O bonds over C=C bonds. One of several impressive traits of this catalyst system is the fast rate and high *ee*. For example, when the pre-catalyst $Ru(Cl)_2$((*S*)-tolBINAP)((*S*,*S*)-DPEN) was added to 45 atm $H_2$ in the presence of a butoxide base at 30 °C, the TOF of acetophenone was $2 \times 10^5\ h^{-1}$ with 80% *ee* [68]. While it is apparent that such systems also operate through an ionic mechanism, Noyori uses the term "metal–ligand bifunctional catalysis" to generally refer to systems that operate by hydride transfer to an outer-sphere molecule [69]. This outer-sphere mechanism is identical to that proposed for the Shvo ruthenium system where the L group (a ketone in Shvo's system) is replaced by an amine in Noyori's catalyst system (Scheme 8).

Extensive mechanistic work by Morris and co-workers [70–72] and Noyori and co-workers [73,74] focused on elucidating the structure and mechanism of the active catalysts involved. The presence an unsubstituted diamine was found to be critical, and the catalysts were found to be ineffective when diamines without NH groups were used [75]. The nature of the so-called "NH-effect" has been widely investigated and is proposed to stabilize an incoming ketone by forming an intermediate like that shown below. Such an intermediate explains the selectivity of polar C=O bonds over C=C bonds [76] (Fig. 12).

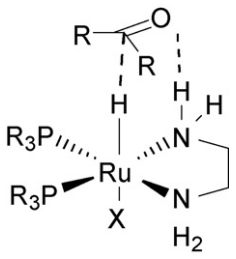


Fig. 12. Proposed intermediate involving the NH-effect in the hydrogenation of a ketone.

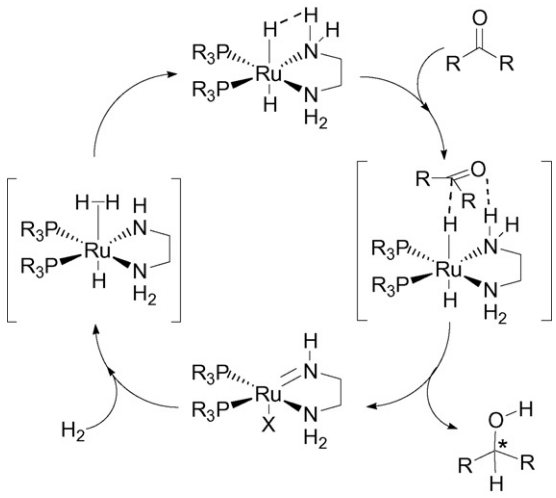

Scheme 9. Morris' proposed pathway for the hydrogenation of ketones by Ru(diamine)(diphosphine)$(H)_2$ complexes.

Subsequent mechanistic work by the Morris group reformulated the active catalyst as a ruthenium dihydride formed by the heterolytic cleavage of $H_2$ [70]. Using deuterium isotope experiments, they found that the rate of hydrogenation decreased when using $D_2$ instead of $H_2$, and they attributed this observation to the decreased acidity of an $\eta^2$-$D_2$ complex compared to an $\eta^2$-$H_2$ complex. Furthermore, they suggested that deprotonation of coordinated dihydrogen by a transiently formed amido ligand is the rate-determining step of the hydrogenation reaction. Their proposed mechanism is shown in Scheme 9 [70–72].

An alternative pathway involving cationic intermediates has also been proposed to be active when the hydrogenation is performed in protic solvents in the absence of exogenous base [73], although an $\eta^2$-$H_2$ complex is still a key intermediate in this pathway.

One of several noteworthy features of the Noyori and Morris mechanisms is that the heterolytic activation of $H_2$ is proposed to be a critical step in catalyzing the asymmetric hydrogenation of ketones and imines. It is noted that several further examples of an $\eta^2$-$H_2$ complex mediating reactivity by an ionic mechanism are known and proposed, such as the hydrogenation of carbon dioxide to formic acid [77,78] using a dihydrogen complex, as well as numerous *aqueous* selective hydrogenation catalysts [35,40,79].

### 3.3.6. Hydrogenase enzymes

The hydrogenase enzymes mediate the conversion of protons and electrons to $H_2$ (Eq. (7)) with impressive efficiency [80]. The physiological role played by hydrogenase enzymes allows $H_2$ to be used as an energy source to drive ATP formation via ATPase or to contribute to acetylCoA synthesis [81]. Additionally, hydrogenase enzymes reclaim the $H_2$ formed as a byproduct in the fixation of $N_2$ to ammonia by nitrogenase [82]. One direction that has been explored extensively to exploit this function is the construction of synthetic models of the active site of Fe–Fe and Fe–Ni hydrogenase enzymes with the goal of synthesizing a viable catalyst for $H_2$ production [83–86]. Such models exploit key structural features found in the enzyme active site, and for the H-cluster (the most widely modeled site), this

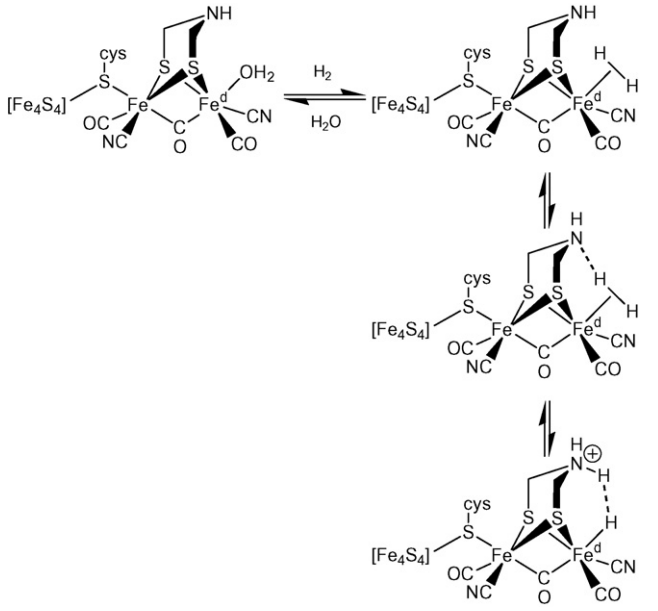

Fig. 13. Proposed intermediates in the hydrogenase-mediated activation of $H_2$.

involves a binuclear iron core featuring three CO ligands, two $CN^{-1}$ ligands, and a thiolate bridging from the $Fe_4S_4$ cluster [87,88].

$$H_2 \rightleftharpoons 2H^+ + 2e^- \quad (7)$$

From a mechanistic standpoint, the intermediates involved in conversion of $H^+$ to $H_2$ are unusual (Fig. 13). In particular, a noteworthy feature of the mechanism is the competitive ability of water, $H_2$ and hydrides to coordinate to an iron center. Although several pathways have been proposed for the conversion of $H_2$ to $H^+$, a common feature is the likely coordination and subsequent heterolytic cleavage of dihydrogen at an iron center [85]. This reaction is likely facilitated either by an amine of the proposed azadithiolate cofactor [88], exogenous water [39], thiolate [89], or another base [90]. Also noteworthy is the presence of a coordinated hydride and an $\eta^2$-$H_2$ ligand coordinated to a metal complex at biological conditions, namely in water (Fig. 13).

X-ray crystallography has provided key insights into the mechanism of $H_2$ conversion. A reduced form of the diiron core was shown to contain an *empty* coordination site on the distal iron center (denoted in Fig. 13 as $Fe^d$). However, a crystallographic study of the oxidized form of the H-cluster showed that a coordinated water molecule was actually bound to the previously identified "empty" coordination site [88,91]. Additionally, introduction of CO to the oxidized form resulted in the substitution of the water molecule by CO and subsequent inhibition at the distal site as determined spectroscopically [92] and crystallographically [93]. Taken together, these results provide good evidence that the site of $H_2$ production/activation is likely on the distal iron center and that, during catalysis, $H_2$ likely displaces coordinated water [38]. Given the importance of the $H_2$ conversion pathway, it is a worthwhile pursuit to understand some of the underlying reactivity trends associated with this rather elusive class of complexes, namely water-soluble and stable M–$H_2$

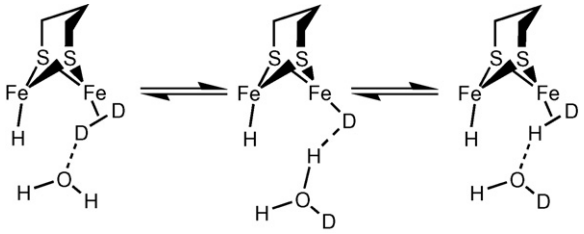

Scheme 10. Proposed intermediates in the hydrogenase-catalyzed H/D exchange reaction mediated by $H_2O$. Ligands other than the hydrides and propanedithiolate bridge have been removed for clarity.

and M–H complexes featuring the heterolytic cleavage of $H_2$ as a key reactivity trait.

### 3.3.7. H/D exchange reactivity

A common reaction of most $H_2$ complexes is their ability to affect H/D exchange reactions between $H_2$ and $D_2$ or $H_2$ and $D^+$. The exchange process has been suggested to occur by one of many possible exotic yet computationally viable routes (p. 121, Ref. [2]). However, the most common pathway likely involves heterolytic cleavage of $H_2$ (Eq. (8)) [42]. In order for H/D exchange to occur efficiently by this route, the p$K_a$ of the $H_2$ ligand and the protonated base must be similar.

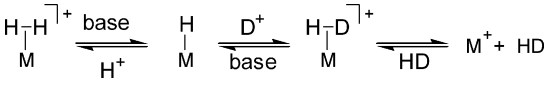

(8)

The H/D exchange reaction is an important feature of nitrogenase and hydrogenase metalloenzymes [94–97] and is one of the requisites for a functional hydrogenase mimic [39,98,99]. In this regard, Darensbourg showed that structural analogues of the hydrogenase enzyme carried out H/D exchange between $H_2$ and $D_2$ and also $H_2/D_2O$ mixtures [90]. It was also noted that the process was not mediated solely by a metal hydride in the $D_2O$-assisted case because replacement of the hydride by a thiolate still gave H/D exchange. However, without the presence of adventitious water, H/D exchange did not occur, and therefore the mechanism in that case is likely due to binuclear cooperation between the two iron sites. Suggested pathways were proposed for both exchange reactions, and the $H_2O$-assisted pathway is shown in Scheme 10.

Several groups have exploited the H/D exchange reactivity of $\eta^2$-$H_2$ complexes for the purpose of selective deuteration of organic molecules using $D_2O$ or $CH_3OD$ as a deuterium source. For instance, Dahlenburg and Gotz reported an unusual example of an iridium complex that activates $H_2$ heterolytically, yet hydrogenates ketones through a classic hydride insertion mechanism (Fig. 14) [100]. The hydrogenation of several ketones was achieved with nearly a 1:1 mixture of deuterium incorporation at the carbonyl carbon.

The proposed mechanism involved an equilibrium between the dihydrogen amido complex and a dihydride amine species (Fig. 15). In this reaction, the dihydrogen complex catalyzed the H/D exchange between $H_2$ and $D_2$ or $H_2$ and $D^+$.

Lau and co-workers recently reported another example of using an H/D exchange reaction of an $\eta^2$-$H_2$ complex to install

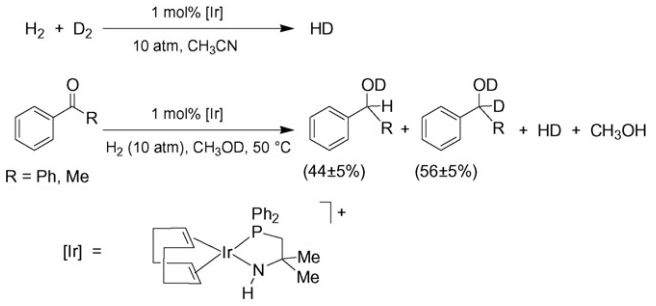

Fig. 14. Catalytic H/D$^+$ exchange and the subsequent hydrogenation of ketones.

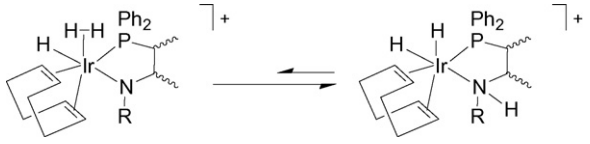

Fig. 15. Proposed equilibrium between an isomeric dihydrogen amido and a dihydride amine pair.

deuterium [34]. The pre-catalyst $TpRu(PPh_3)(CH_3CN)H$ was reacted with $D_2O$ to form a proposed Ru(HD) intermediate species prior to transferring the deuterium to an organic substrate via a C–H activation process (Fig. 16).

Various ethers and aromatic substrates were tested for deuterium incorporation and benzene was found to give the highest deuteration (27%) at 0.4 mol% catalyst loading. Interestingly, although substrate solubility was an important issue to consider when exchanging aliphatic R–H with deuterium from $D_2O$, the highest degree of deuteration was obtained when an immiscible solvent system (water/benzene) was used, compared to highly miscible water/THF or water/dioxane solutions. The $TpRu(PPh_3)(CH_3CN)H$ complex was also found to catalyze the H/D exchange between $H_2$ and various deuterated solvents (THF-$d_8$, benzene-$d_6$, and diethyl ether-$d_{10}$) to give mixtures of HD and $D_2$. Thus, the $TpRu(PPh_3)(CH_3CN)H$ system presents an intriguing alternative to H/D exchange by traditional heterolytic mechanisms involving polar substrates.

Bianchini reported another example of an unusual H/D exchange reaction involving a tripodal phosphine osmium dihydrogen hydride complex (Scheme 11) [101]. When deuterated acetone was used as a solvent, deuterium incorporation into the $H_2$ ligand was observed. The reaction was proposed to proceed via a keto-enol tautomerization of acetone because the p$K_a$ of the $H_2$ ligand is thought to be more acidic than acetone (p$K_a$ = 26 in DMSO). (Note that a similar complex, $[Os(DPPE)_2(H_2)H]BF_4$, has an experimentally determined p$K_a$ value of 12.7 in THF [102].) The H/D exchange reaction with acetone-$d_6$ was also noted to occur with *trans*-$[Ru(DPPE)_2(H_2)Cl]PF_6$ [103]. Within

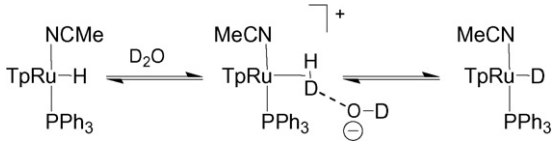

Fig. 16. Proposed equilibrium between the ruthenium hydride and a ruthenium dihydrogen complex.

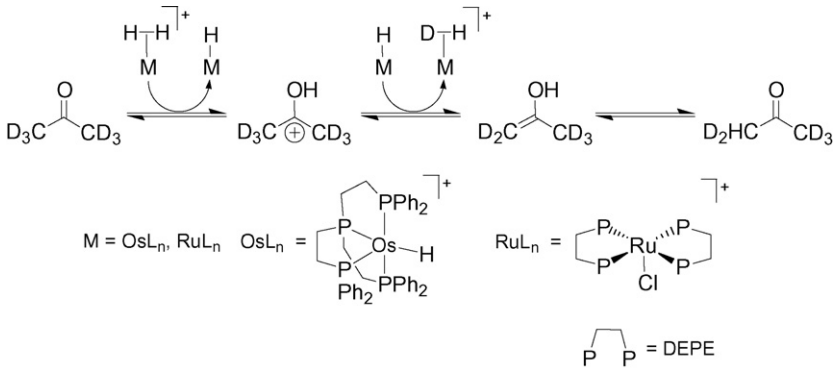


Scheme 11. Proposed mechanism for the H/D exchange with acetone-$d_6$ mediated by a ruthenium or osmium $\eta^2$-$H_2$ complex.

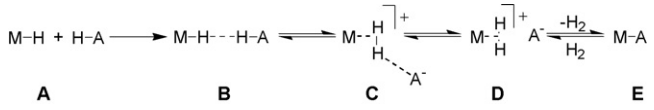


Scheme 12. Proposed intermediates in the proton transfer of a metal hydride (MH) and an acid (AH).

20 min of dissolution into acetone-$d_6$ the H/D isotopolog formed and within a few hours complete deuterium incorporation was noted. In this case, a mechanism was not proposed for the H/D exchange. However, it is likely to proceed in a manner analogous to the osmium species because the $H_2$ ligand is moderately acidic ($pK_a = 6$, pseudo-aqueous scale).

## 4. Proton transfer reactions involving $\eta^2$-$H_2$ complexes

All of the reactions shown above that involve the heterolytic cleavage of $H_2$ can generally be classified as proton transfer reactions. Proton transfer pathways involving the transfer of a proton to a metal hydride play a key role in catalytic ionic hydrogenations, the reduction of $H^+$ to $H_2$, and H/D exchange reactions [104]. Accordingly, significant experimental and theoretical research has been devoted to uncover intermediates and gain mechanistic insight into the elementary steps involved in proton transfer reactions. The stepwise proton transfer to a metal hydride shown in Scheme 12 is the generally accepted route for these reactions.

Note that species **A**, **D**, and **E** are discrete and well-characterized species. Species **B** and **C** represent the key intermediates that have remained elusive for many years. In an effort to understand these key intermediates, Crabtree and co-workers [105] and Morris and co-workers [106] independently discovered the capacity of a metal hydride to accept a hydrogen bond from an appropriate hydrogen bond donor. This finding revealed new bonding possibilities and caused many mechanistic questions to be readdressed. The field of dihydrogen bonding (also known as "protonic/hydridic" bonding) has been extensively reviewed [107–111], so this topic will not be covered in detail here. To further elucidate the presence of intermediates along the proton transfer pathway, Chaudret showed that a dynamic equilibrium involving proton transfer exists in solution between a hydride and a dihydrogen complex in the presence of an acidic alcohol (Fig. 17) [112]. Further studies have since

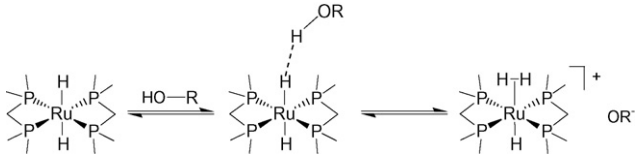


Fig. 17. The dynamic equilibrium between a hydride and a dihydrogen complex observed by Chaudret and co-workers [112].

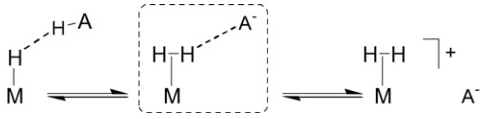

Fig. 18. Proposed intermediate contact ion pair (hashed box).

confirmed the generality of these equilibria in other systems [113–115].

An intermediate species between the hydrogen bonded alcohol and the discrete dihydrogen complex (species C) was proposed to be directed by electrostatic forces as a contact ion pair [116,117] or alternatively as a hydrogen-bonded species with dihydrogen (Fig. 18).

### 4.1. Dihydrogen hydrogen bonding (DHHB)

The hydrogen bonding interaction between a coordinated $H_2$ ligand and a hydrogen bond acceptor has been proposed as an intermediate in H/D exchange reactions (see Scheme 10 for an example) and other variants of proton transfer [34,90]. Among the first crystallographically identified instances that potentially contain a hydrogen bonded $\eta^2$-$H_2$ ligand are an iron phosphine complex, $Fe(H)_2(H_2)(PEtPh_2)_3$ (Fig. 19) [118], and an iridium phosphine complex, $Ir(\eta^2\text{-}H_2)H(Cl)_2(P^iPr_3)_2$ (Fig. 20) [119]. With the iron species, the $H_2$ ligand was located by neutron

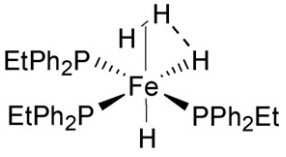


Fig. 19. The *cis*-effect in the $Fe(H)_2(H_2)(PEtPh_2)_3$ complex determined by neutron diffraction.

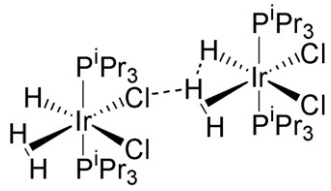


Fig. 20. The crystal packing of the Ir($\eta^2$-H$_2$)H(Cl)$_2$(P$^i$Pr$_3$)$_2$ complex exhibits intermolecular close contacts between a *cis*-hydride ligand and a nearby chloride ligand.

diffraction and found to be unusually staggered with respect to the P–Fe–P and Fe–H axes. A computational study revealed an interaction between a *cis*-hydride and dihydrogen ligands. This was subsequently called the "*cis*-effect" and can be loosely described as an interaction of the hydride σ-orbital with the σ* orbital of the coordinated $H_2$ (Fig. 19).

The barrier to $H_2$ rotation was probed by low-frequency inelastic neutron scattering spectroscopy and was found to be abnormally low. The low barrier was rationalized by considering the stabilizing interaction between $H_2$ and the *cis* Fe–H bond that served to decrease the strength of the Fe–$H_2$ back-bonding contribution. Further studies of the *cis*-effect on an $H_2$ ligand were reported for an osmium complex, which showed that this interaction lengthens the H–H bond distance when the *cis* ligand is changed and follows the order H > F > Cl > $H_2O$ [120].

The Ir($\eta^2$-H$_2$)H(Cl)$_2$(P$^i$Pr$_3$)$_2$ complex was shown in the solid state to have close contacts between an $\eta^2$-$H_2$ ligand of one molecule and a chloride ligand of another molecule and a *cis*-hydride [119]. However, due to the large size of the phosphine ligands and the fact that the complex does not retain its $\eta^2$-$H_2$ ligand in solution [121], the actual driving force for the molecular association is unclear and might be due to crystal-packing effects rather than hydrogen bonding.

There are a several examples of crystal structures of dihydrogen complexes that exhibit close contacts to a counterion and potentially are associated by dihydrogen hydrogen bonding interactions [122,123]. Notably, the acidic *trans*-[Os(DPPE)$_2$(H$_2$)(CH$_3$CN)][BF$_4$]$_2$ complex was shown to contain a $BF_4^-$ group in close proximity to the coordinated $H_2$ ligand (2.365 Å) (Fig. 21). The close proximity of $BF_4^-$ was presumed to facilitate the mobility of the proton [123].

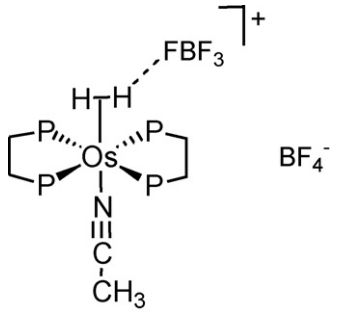


Fig. 21. The solid-state structure of the *trans*-[Os(DPPE)$_2$(H$_2$)(CH$_3$CN)][BF$_4$]$_2$ complex exhibits intermolecular close contacts to the $BF_4^-$ counterion.

Similar ion pairing phenomena were proposed to facilitate proton transfer in other systems. For example, the kinetics of deprotonation of *trans*-[Fe(DPPE)$_2$H(H$_2$)]$^+$ by $NEt_3$ were shown to be governed by the counterion [124]. In this reaction, the anion was found to facilitate the separation of the reaction products through the formation of a stable ion pair. This finding conflicted with the previously proposed hypothesis that the role of the ion pair was to mobilize a proton in an otherwise sterically congested area [123].

Although H-bonding may be responsible for the crystalline arrangement of these associated complexes, other factors such as steric and electronic repulsion and crystal-packing forces are likely to give similar energetic stabilization. The few instances in which a hydrogen bond to a coordinated $\eta^2$-$H_2$ ligand is proposed in solution involve a counterion acting as the H-bond acceptor [117,125–128]. Thus, the driving force for these associations in solution may be driven by the formation of a tight ion pair instead of by hydrogen bonding interactions. To clarify the nature of the interactions of $H_2$ with appropriate H-bond acceptors, several computational reports have shown that intermolecular hydrogen bonding to a coordinated $H_2$ is possible [33,37,121,128–131] in spite of a report stating that intermolecular H-bonding in solution is unlikely because the $H_2$ would be screened from the surroundings by the shell of co-ligands [132].

We recently reported the identification of intermolecular DHHB in the solution phase [31]. Specifically, the water-soluble *trans*-[Ru(DMeOPrPE)$_2$(H$_2$)H]$^+$ complex (DMeOPrPE = 1,2-bis(dimethoxypropylphosphino)ethane) was spectroscopically shown to participate in DHHB with the potent H-bond acceptor pyridine N-oxide. Three tests unambiguously established the presence of DHHB in this complex. First, downfield shifts of the $\eta^2$-$H_2$ resonance were noted in the $^1$H NMR spectrum upon titration of an appropriate acceptor molecule (acetone and pyridine N-oxide) into a non-aqueous solution of the complex. The shape of the binding isotherm (as well as the association constant, $K_a$) was dependent on the identity of the acceptor. (The association constant for pyridine N-oxide was four times as large as that for acetone.) A second test employed a solvatochromic H-bond probe (4-nitropyridine N-oxide) that has a $\lambda_{max}$ that is sensitive to H-bond donors. Thus, DHHB was indicated in the *trans*-[Ru(DMeOPrPE)$_2$(H$_2$)H]$^+$ complex by a hypsochromic shift in the $\lambda_{max}$ of the probe molecule (Scheme 13, right side). An analogous experiment with the carbonyl-substituted complex *trans*-[Ru(DMeOPrPE)$_2$(CO)H]$^+$ gave no change in the $\lambda_{max}$ of the probe molecule (Scheme 13, right side). Thus, substitution of the $\eta^2$-$H_2$ ligand by CO showed that the association was specific to the $\eta^2$-$H_2$ ligand and not merely a result of association with the coordination complex.

A third test confirming DHHB came from a study of the rotational dynamics of a probe molecule, pyridine N-oxide-$d_5$. Using $^2$H NMR spectroscopy, the solution dynamics of the probe molecule in the presence of the *trans*-[Ru(DMeOPrPE)$_2$(H$_2$)H]$^+$ complex and its carbonyl analogue were investigated. The addition of the large $\eta^2$-$H_2$ complex (relative to the pyridine N-oxide probe molecule) caused a substantial *increase* in the rotational correlation time ($\tau_c$) of the probe molecule. This increase is a result of an increase in the

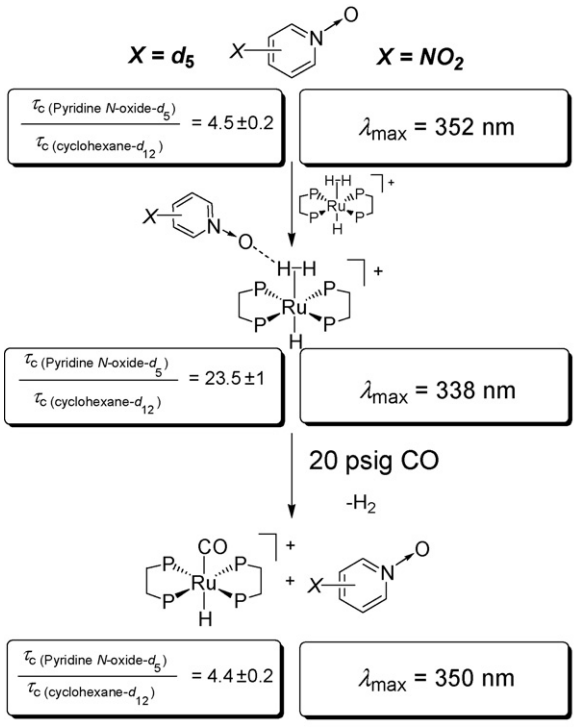


Scheme 13. Addition of the *trans*-$[Ru(DMeOPrPE)_2(H_2)H]^+$ complex to pyridine N-oxide probe molecules causes changes in the rotational correlation time ($\tau_c$) and the $\lambda_{max}$. In the $\tau_c$ experiment, note that cyclohexane-$d_{12}$ was used as an internal standard to normalize for the effects of solvent viscosity.

effective volume and is consistent with the formation of an H-bonded adduct. When the $H_2$ ligand was replaced by CO, the effect of adding the $H_2$ complex was reversed and *trans*-$[Ru(DMeOPrPE)_2(CO)H]^+$ caused no increase in the $\tau_c$ of the probe molecule (Scheme 13, left side). Taken together, all three tests suggest that intermolecular DHHB is possible to a neutral acceptor.

These and other studies give a rationale for studying DHHB in solution as a way to gain insight into the nature of the interaction as well as to determine how such interactions change the reactivity.

The DHHB interaction can be loosely described by the orbital description shown in Fig. 22.

It is important to note that the M–($H_2$) bond strength is significantly affected by the M–$d_\pi \rightarrow \sigma^*$ back-bonding contribution [2,133]. The H-bond acceptor likely populates the $\sigma^*$ acceptor orbital of $H_2$. Thus, upon participation in DHHB interactions,

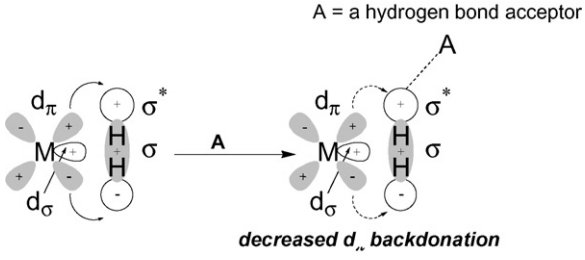


Fig. 22. The proposed orbital diagram showing the effect of DHHB on metal backdonation into the $\sigma^*$ orbitals of the $H_2$.

there are two likely consequences to the M–($H_2$) bond; a lengthening of the H–H bond distance and as well as a concomitant lengthening of the M–($H_2$) bond distance. Unfortunately, the competition between these two effects may offset the ability to directly observe the effect of H-bonding on the H–H distance in $\eta^2$-$H_2$ complexes.

The increased lability of an $H_2$ complex is likely to be one of the most important consequences of DHHB. Furthermore, because several proposed intermediates in the hydrogenase-mediated reduction of protons feature DHHB species (Fig. 13) [38,85], it is possible that biological enzymes may have evolved to explicitly include this interaction in their active site structures.

## 5. Nuclear magnetic resonance characterization of $\eta^2$-$H_2$ complexes

The characterization of $\eta^2$-$H_2$ complexes typically relies on measuring the H–H bond distance because it is a good indicator of the extent of π-back-bonding, and thus of $H_2$ activation [12]. Several techniques are available to examine the H–H bond distance [2,17]. Because hydrogen atoms are typically X-ray silent, X-ray diffraction methods are generally not amenable to H–H bond length determinations. Nevertheless, crystallographic determinations are possible using neutron diffraction. However, this technique requires significantly larger crystals than X-ray crystallography and access to a neutron source. As a convenient alternative to diffraction, NMR spectroscopy has been extensively used to measure H–H bond distances. Because of the omnipresence of NMR spectrometers in most research institutions, techniques based on solution-phase characterization have emerged that allow an H–H bond distance to be straightforwardly measured using one of several solution-phase or solid-state NMR methods. The prominent solution-phase NMR methods are outlined below.

### 5.1. HD-coupling as a probe of the $d_{HH}$

The close proximity of the two hydrogen atoms in an $H_2$ complex allows significant interaction between the two nuclei. A consequence of this interaction is manifested in the HD coupling constant in the $^1$H NMR spectra of HD complexes (Fig. 23). In fact, a key piece of evidence supporting the structural assignment of the first dihydrogen complex was the large HD coupling constant of 33.5 Hz [1]. Isotopic substitution of one of the hydrogen atoms by deuterium forms the HD isotopolog, which has a characteristic 1:1:1 triplet because deuterium has a spin of 1. Free HD gas has a $J_{HD}$ of 43 Hz, and accordingly, this is the upper limit of an HD coupling constant. Substitution can be achieved by treating a coordinatively unsaturated complex with HD gas directly [2]. More commonly, synthesis proceeds by protonation of a metal deuteride or by treating a metal hydride with a deuterated acid or an exchangeable deuterium source such as an alcohol.

Several empirical relationships that correlate the measured $J_{HD}$ with the $d_{HH}$ in a given molecule have been found, the first of which was given by Morris and co-workers [134]. A linear relationship was discovered when the $d_{HH}$ was plotted against

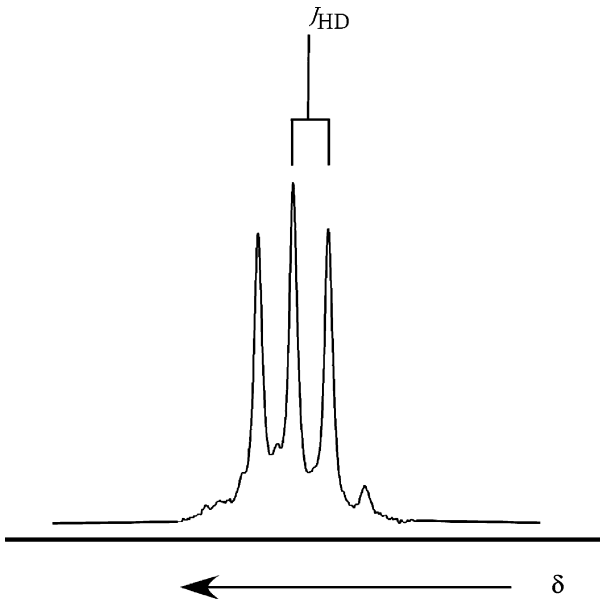


Fig. 23. A typical high field $^1$H NMR spectrum of an HD isotopolog of an $\eta^2$-$H_2$ complex.

the measured $J_{HD}$ value (Eq. (9)). Morris used a large set of distances that included uncorrected neutron data, X-ray diffraction data, distances obtained by solid-state NMR measurements, and corrected neutron data [134]:

$$d_{HH} = 1.42 - [0.0167(J_{HD})]\ \text{Å} \quad (9)$$

A slightly different variation was constructed by Heinekey who used a slightly smaller data set that included H–H distances obtained from solid-state NMR methods and corrected neutron diffraction data [135]:

$$d_{HH} = 1.44 - [0.0168(J_{HD})]\ \text{Å} \quad (10)$$

Considering the uncertainty in obtaining the $J_{HD}$ (±0.3 Hz), the error associated with these measurements is estimated to be ±0.005 Å [136].

Both of these correlations have been successfully used for the characterization of "short" dihydrogen complexes ($d_{HH}$ < 1.1 Å). However, the correlation breaks down for "stretched" or *elongated* $\eta^2$-$H_2$ complexes ($d_{HH}$ = 1.1–1.5 Å). A more recent adaptation of the linear equation relating the $J_{HD}$ with the $d_{HH}$ was provided by Gusev [121], who reported that the new relationship yielded a slightly better fit than Morris' original relationship, although the linear relationship still breaks down at distances greater than 1.3 Å (Fig. 24):

$$d_{HH} = 1.47 - [0.0175(J_{HD})]\ \text{Å} \quad (11)$$

To establish a correlation that was accurate for both short and elongated $H_2$ distances, Limbach and Chaudret used an approach based on the bond-valence bond-length concept [137]. They based their model on a relationship given by Hush [138] who showed that the $J_{HD}$ is proportional to the H–H bond order, $p_{HH}$. Because free $H_2$ has a $J_{HD}$ value of 43 Hz, Hush's relationship is

$$J_{HD} = 43 p_{HH} \quad (12)$$

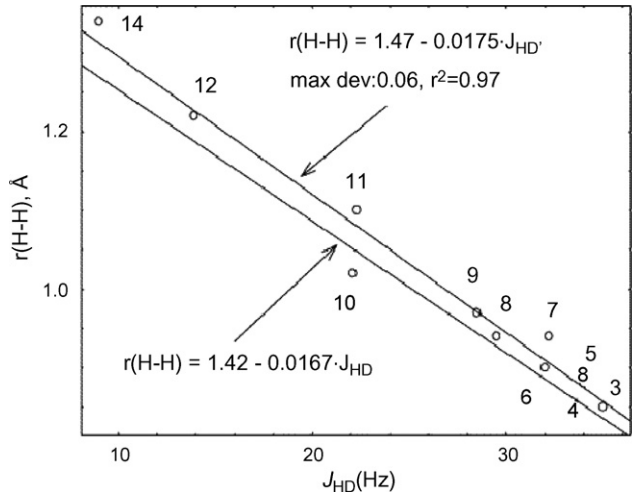


Fig. 24. The H–H bond distance ($r_{H–H}$) up to 1.3 Å as a function of $J_{HD}$ showing fits using Morris' and Gusev's linear relationship. Reprinted with permission from Ref. [121]. Copyright 2004 American Chemical Society.

The correlation proposed by Limbach and Chaudret is

$$J_{HD} = 43 \exp\left(\frac{0.74 - d_{HH}}{0.404}\right) - 2.81\left(1 - \exp\left(\frac{0.74 - d_{HH}}{0.404}\right)\right)^2 \quad (13)$$

Heinekey further refined this correlation and was able to obtain a better fit (Fig. 25) with experimentally determined H–H bond distances [139]:

$$J_{HD} = 43 \exp\left(\frac{0.74 - d_{HH}}{0.494}\right) - 3.04\left(1 - \exp\left(\frac{0.74 - d_{HH}}{0.494}\right)\right)^2 \quad (14)$$

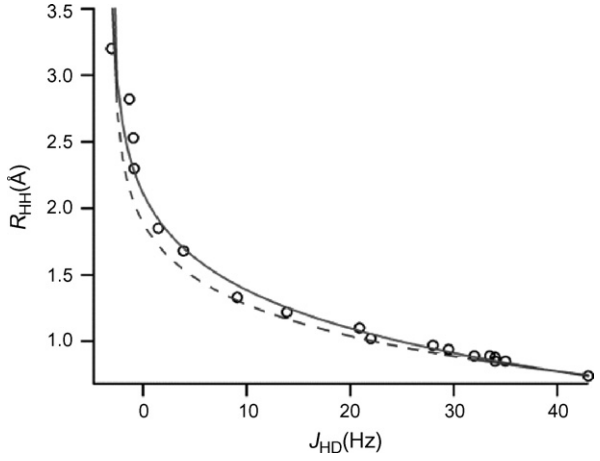


Fig. 25. The H–H bond distance ($R_{HH}$) as a function of $J_{HD}$. The dashed curve represents the fit from Limbach and Chaudret's relationship given in Eq. (13), and the solid curve represents a fit using Heinekey' modifications as given in Eq. (14). Reprinted with permission from Ref. [139]. Copyright 2004 American Chemical Society.

### 5.2. H–T spin–spin coupling

Heinekey showed that isotopic substitution using tritium is a more precise technique to probe the H–H bond distance. Tritium ($^3$H) has a nuclear spin of 1/2 and a gyromagnetic ratio almost seven times as large as $^2$H. Accordingly, H–T couplings are much larger than H–D coupling constants, and thus the detection of small changes in the coupling constant are more reliable when using $J_{HT}$ compared to $J_{HD}$. Heinekey has been the main advocate of this technique and estimated the experimental uncertainty in the measurement of $J_{HT}$ as ±0.4 Hz. Thus, the error associated with the $d_{HH}$ determination is estimated to be ±0.001 Å [136]. From an experimental standpoint, the use of tritium has many drawbacks, the major being the radioactive nature of the $^3$H isotope. Consequently, most inorganic chemistry groups are not equipped to use tritium without specialized equipment and training, and this has translated into limited use of this otherwise powerful technique.

### 5.3. $^1$H NMR dipolar relaxation as a tool for identification of $H_2$ complexes

For the same reason that the $J_{HD}$ correlation described above finds utility in H–H bond distance characterization, the measurement of relaxation rates of an $\eta^2$-$H_2$ ligand has become an important characterization tool to evaluate an H–H bond distance. The relaxation rate of a perturbed nucleus is inversely related to the spin–lattice, or the $T_1$, relaxation mechanism:

$$\text{relaxation rate} = R = \frac{1}{T_1} \tag{15}$$

The relaxation rate is comprised of at least four contributing relaxation components:

$$R = R_{\text{dipolar}} + R_{\text{quadrupolar}} + R_{\text{CSA}} + R_{\text{other}} \tag{16}$$

where CSA represents the chemical shift anisotropy. For dihydrogen complexes, the dipolar term dominates because the excited nuclei can effectively relax through an adjacent H-atom. Due to the close proximity of the two excited nuclei, $H_2$ complexes have extremely short $T_1$ values because of efficient dipolar relaxation. The so-called dipole–dipole relaxation has been attributed as the cause of the broad peaks typically associated with $H_2$ complexes [140]. A consequence of a dipolar relaxation mechanism is that the observed $T_1$ value will go through a minimum value at a given temperature [141]. The minimum value occurs when the rate of molecular tumbling in solution matches the Larmor frequency. The equation describing dipolar relaxation is

$$\frac{1}{T_1} = \frac{3\gamma^4\hbar^2}{10r^6}\left[\frac{\tau_c}{1+\tau_c^2\omega^2} + \frac{4\tau_c}{1+4\tau_c^2\omega^2}\right] \tag{17}$$

where $\gamma$ is the gyromagnetic ratio, $\hbar$ the Planck's constant/2π, $r$ the internuclear distance, $\tau_c$ the rotational correlation time, and $\omega$ is the Larmor frequency. In the extreme narrowing limit ($\omega^2\tau_c^2 \ll 1$), the dynamic term in brackets reduces to $5\tau_c$, whereas if $\omega^2\tau_c^2 \gg 1$, the term reduces to $2/\omega^2\tau_c$. Thus, in the extreme narrowing limit, Eq. (17) converts to

$$\frac{1}{T_1} = \left(\frac{3}{2}\right)\frac{\gamma^4\hbar^2}{r^6}(\tau_c) \tag{18}$$

While in the slow molecular motion regime, Eq. (17) simplifies to

$$\frac{1}{T_1} = \left(\frac{3}{5}\right)\frac{\gamma^4\hbar^2}{r^6}\left(\frac{1}{\omega^2\tau_c}\right) \tag{19}$$

This relationship was exploited by Crabtree and Hamilton to empirically correlate the $d_{HH}$ with a measured value of $T_1$ (min) at 250 MHz: for dihydrogen complexes, $T_1 < 80$ ms, while for classical dihydrides, $T_1 > 150$ ms.

Eq. (17) predicts that the $T_1$ will go through a minimum value when the rotational correlation time closely matches the Larmor frequency. By utilizing the minimum value of $T_1$, the influence of $\tau_c$ on the $T_1$ can be neglected and Eq. (17) can be converted into a simpler expression. Thus, in the slow rotation regime (i.e. the H nuclei of the $H_2$ ligand have slow motion relative to the molecular tumbling in solution) the $d_{HH}$ can be approximated by [142,143]:

$$d_{HH} = 5.81\sqrt[6]{\frac{T_1(\text{slow})}{\nu}} \tag{20}$$

where $\nu$ is the spectrometer frequency. A correct treatment of the $T_1$ (min) criteria that correlates with the $d_{HH}$ requires knowledge of the anisotropic contribution to the relaxation. Thus, errors in calculations of the $d_{HH}$ depend on the character of the anisotropy of the $H_2$ rotation. When $H_2$ rotation is very fast and the dipolar H–H vectors are perpendicular to the internal rotational axis, the measured $T_1$ values are maximal [141]:

$$T_1\,(\text{anisotropic}) = 4T_1\,(\text{isotropic}) \tag{21}$$

Accordingly, in the fast motion regime (i.e. $H_2$ rotation is much slower than molecular reorientation) the measured $T_1$ value is four times longer, and Eq. (20) transforms into [144]:

$$d_{HH} = 4.61\sqrt[6]{\frac{T_1\,(\text{fast})}{\upsilon}} \tag{22}$$

A further assessment of the method correlating the H–H bond distance with the measured $T_1$ (min) value was made by Halpern and co-workers [142]. In this treatment, relaxation contributions from other nuclei on the observed $T_1$ are accounted for. For instance, relaxation contributions from nearby spin-active $^{31}$P atoms, *ortho*-CH pendant groups, as well as transition metals with non-negligible gyromagnetic ratios may lead to erroneously measured $T_1$ values. It should be stressed that the measured relaxation rates ($R_{obs}$) are additive and the observed relaxation rate includes all the dipolar contributions as well as relaxation by other mechanisms (Eq. (16)):

$$[R]_{\text{obs}} = \sum_n R \tag{23}$$

A limitation of the $T_1$ method for determining the identity of an unknown hydride is the sensitivity to paramagnetic species [141]. Relaxation by such species can dominate the

overall relaxation process and lead to erroneously measured $T_1$ values. Fortunately, many $H_2$ complexes have low spin $d^6$ configurations (and hence are diamagnetic) and are air-sensitive, so relaxation due to paramagnetic $^3O_2$ is eliminated. Complications can arise, however, if the sample is not pure and contains paramagnetic impurities, or alternatively if the sample undergoes decomposition to an ill-defined paramagnetic species.

Experimentally, the determination of a $T_1$ (min) value for an $H_2$ resonance is straightforward. The spin–lattice time ($T_1$) can be conveniently measured using the inversion-recovery method which relies on a $(RD–180^\circ–\tau–90^\circ–AT)_n$ pulse sequence, where $n$ is the number of accumulations. The system is allowed to evolve for a delay time, $\tau$, which is varied from $\tau < T_1$ to $\tau > 3T_1$. During the delay time, the net $Z$ component of the magnetization returns to its equilibrium value $M_0$ at a rate dependent on $T_1$. The evolution of the inverted peak can be treated with a three-parameter fitting equation to extract the value of $T_1$.

### 5.4. Use of deuterium quadrupolar coupling constants

Another potentially powerful NMR technique has emerged to probe $H_2$ complexes in solution. The deuterium quadrupole coupling constant (DQCC) can be a sensitive measure of changes around a coordinated $\eta^2$-$H_2$ ligand [145,146]. Changes due to the intramolecular motions of $H_2$ are measured by changes in the orientation of the electric field gradient tensors, and this technique has been used to distinguish fast-spinning dihydrogen ligands [147]. The DQCC value can be accessed from complementary information obtained from $^2H$ NMR spectroscopy (correlated to the $^2H$ $T_1$ time) of a $\eta^2$-$D_2$ complex and by theoretical calculations using DFT.

## 6. Summary

Water-soluble and stable $\eta^2$-dihydrogen complexes are an attractive class of compounds that merit investigation into their solution behavior. They are promising candidates as selective catalysts for proton transfer reactions, including hydrogenation reactions proceeding through an *ionic* pathway and H/D exchange reactions. These proton transfer reactions lend themselves to ionizing solvents such as water because they involve a highly charged transition state. Currently, there is a dearth of water-stable dihydrogen complexes. Furthermore, studies governing their solution behavior are lacking.

Some fundamental questions arise when working with aqueous dihydrogen complexes. Specifically, it was not known whether coordinated $H_2$ has the capacity to act as an H-bond donor *intermolecularly* to an appropriate H-bond acceptor such as water in solution. Hydrogen bonding interactions are presumed to mediate proton transfer reactions in water, including the hydrogenase-mediated H/D exchange reaction.

## Acknowledgment

We thank the NSF for funding (NSF-CHE-0452004 and an NSF IGERT fellowship to NKS).

## References

[1] G.J. Kubas, R.R. Ryan, B.I. Swanson, P.J. Vergamini, H.J. Wasserman, J. Am. Chem. Soc. 106 (1984) 451.
[2] G.J. Kubas (Ed.), Metal Dihydrogen and σ-Bond Complexes: Structure, Theory and Reactivity, Kluwer Academic/Plenum, New York, 2001.
[3] R.H. Crabtree, Acc. Chem. Res. 23 (1990) 95.
[4] D.M. Heinekey, W.J. Oldham Jr., Chem. Rev. 93 (1993) 913.
[5] P.G. Jessop, R.H. Morris, Coord. Chem. Rev. 121 (1992) 155.
[6] R.H. Crabtree, Angew. Chem., Int. Ed. Engl. 32 (1993) 789.
[7] G.J. Kubas, Catal. Lett. 104 (2005) 79.
[8] C. Bianchini, M. Peruzzini, in: M. Peruzzini, R. Poli (Eds.), Recent Advances in Hydride Chemistry, Elsevier, Amsterdam, 2001, p. 271.
[9] E.T. Papish, M.P. Magee, J.R. Norton, in: M. Peruzzini, R. Poli (Eds.), Recent Advances in Hydride Chemistry, Elsevier, Amsterdam, 2001, p. 39.
[10] R. Noyori, Acta Chem. Scand. 50 (1996) 380.
[11] R. Noyori, T. Ohkuma, Pure Appl. Chem. 71 (1999) 1493.
[12] G.J. Kubas, J. Organomet. Chem. 635 (2001) 37.
[13] K. Abdur-Rashid, T.P. Fong, B. Greaves, D.G. Gusev, J.G. Hinman, S.E. Landau, A.J. Lough, R.H. Morris, J. Am. Chem. Soc. 122 (2000) 9155.
[14] M.S. Chinn, D.M. Heinekey, N.G. Payne, C.D. Sofield, Organometallics 8 (1989) 1824.
[15] E. Rocchini, A. Mezzetti, H. Rueegger, U. Burckhardt, V. Gramlich, A. Del Zotto, P. Martinuzzi, P. Rigo, Inorg. Chem. 36 (1997) 711.
[16] G. Jia, C.P. Lau, Coord. Chem. Rev. 190–192 (1999) 83.
[17] R.H. Morris, Can. J. Chem. 74 (1996) 1907.
[18] T. Li, A.J. Lough, C. Zuccaccia, A. Macchioni, R.H. Morris, Can. J. Chem. 84 (2006) 164.
[19] P.J. Brothers, Prog. Inorg. Chem. 28 (1981) 1.
[20] R.H. Morris, in: M. Peruzzini, R. Poli (Eds.), Recent Advances in Hydride Chemistry, Elsevier, Amsterdam, 2001, p. 1.
[21] G.J. Kubas, Adv. Inorg. Chem. 56 (2004) 127.
[22] J. Malin, H. Taube, Inorg. Chem. 10 (1971) 2403.
[23] Z.W. Li, H. Taube, J. Am. Chem. Soc. 113 (1991) 8946.
[24] T. Hasegawa, Z. Li, S. Parkin, H. Hope, R.K. McMullan, T.F. Koetzle, H. Taube, J. Am. Chem. Soc. 116 (1994) 4352.
[25] T. Hasegawa, Z. Li, H. Taube, Chem. Lett. (1999) 7.
[26] W.D. Harman, H. Taube, J. Am. Chem. Soc. 112 (1990) 2261.
[27] Z.W. Li, H. Taube, Science 256 (1992) 210.
[28] N. Aebischer, U. Frey, A.E. Merbach, Chem. Commun. (1998) 2303.
[29] J.D. Gilbertson, N.K. Szymczak, D.R. Tyler, Inorg. Chem. 43 (2004) 3341.
[30] J.D. Gilbertson, N.K. Szymczak, J.L. Crossland, W.K. Miller, D.K. Lyon, B.M. Foxman, J. Davis, D.R. Tyler, Inorg. Chem. 46 (2007) 1205.
[31] N.K. Szymczak, L.N. Zakharov, D.R. Tyler, J. Am. Chem. Soc. 128 (2006) 15830.
[32] N.K. Szymczak, D.R. Tyler, unpublished observations.
[33] H.S. Chu, Z. Xu, S.M. Ng, C.P. Lau, Z. Lin, Eur. J. Inorg. Chem. (2000) 993.
[34] C.W. Leung, W. Zheng, D. Wang, S.M. Ng, C.H. Yeung, Z. Zhou, Z. Lin, C.P. Lau, Organometallics 26 (2007) 1924.
[35] G. Kovacs, L. Nadasdi, G. Laurenczy, F. Joo, Green Chem. 5 (2003) 213.
[36] A. Rossin, G. Kovacs, G. Ujaque, A. Lledos, F. Joo, Organometallics 25 (2006) 5010.
[37] G. Kovacs, G. Schubert, F. Joo, I. Papai, Organometallics 24 (2005) 3059.
[38] J. Huhmann-Vincent, B.L. Scott, G.J. Kubas, Inorg. Chim. Acta 294 (1999) 240.
[39] I.P. Georgakaki, M.L. Miller, M.Y. Darensbourg, Inorg. Chem. 42 (2003) 2489.
[40] B.J. Frost, C.A. Mebi, Organometallics 23 (2004) 5317.
[41] M.A. Esteruelas, L.A. Oro, Chem. Rev. 98 (1998) 577.
[42] A.C. Albeniz, D.M. Heinekey, R.H. Crabtree, Inorg. Chem. 30 (1991) 3632.
[43] M. Hidai, Y. Nishibayashi, in: M. Peruzzini, R. Poli (Eds.), Recent Advances in Hydride Chemistry, Elsevier, Amsterdam, 2001, p. 117.

[44] R.M. Bullock, Chem. Eur. J. 10 (2004) 2366.
[45] D.N. Kursanov, Z.N. Parnes, N.M. Loim, Synthesis (1974) 633.
[46] P.L. Gaus, S.C. Kao, K. Youngdahl, M.Y. Darensbourg, J. Am. Chem. Soc. 107 (1985) 2428.
[47] D.H. Gibson, Y.S. El-Omrani, Organometallics 4 (1985) 1473.
[48] R.M. Bullock, M.H. Voges, J. Am. Chem. Soc. 122 (2000) 12594.
[49] J.-S. Song, D.J. Szalda, R.M. Bullock, Organometallics 20 (2001) 3337.
[50] G. Jia, R.H. Morris, J. Am. Chem. Soc. 113 (1991) 875.
[51] G. Jia, R.H. Morris, Inorg. Chem. 29 (1990) 581.
[52] T.-Y. Cheng, R.M. Bullock, Organometallics 21 (2002) 2325.
[53] T.-Y. Cheng, B.S. Brunschwig, R.M. Bullock, J. Am. Chem. Soc. 120 (1998) 13121.
[54] R.M. Bullock, J.-S. Song, D.J. Szalda, Organometallics 15 (1996) 2504.
[55] E.T. Papish, F.C. Rix, N. Spetseris, J.R. Norton, R.D. Williams, J. Am. Chem. Soc. 122 (2000) 12235.
[56] B.F.M. Kimmich, P.J. Fagan, E. Hauptman, R.M. Bullock, Chem. Commun. (2004) 1014.
[57] H. Guan, M. Iimura, M.P. Magee, J.R. Norton, G. Zhu, J. Am. Chem. Soc. 127 (2005) 7805.
[58] H. Guan, S.A. Saddoughi, A.P. Shaw, J.R. Norton, Organometallics 24 (2005) 6358.
[59] H. Guan, M. Iimura, M.P. Magee, J.R. Norton, K.E. Janak, Organometallics 22 (2003) 4084.
[60] M.P. Magee, J.R. Norton, J. Am. Chem. Soc. 123 (2001) 1778.
[61] Y. Nishibayashi, I. Takei, M. Hidai, Angew. Chem., Int. Ed. 38 (1999) 3047.
[62] I. Ojima, M. Nihonyanagi, T. Kogure, M. Kumagai, S. Horiuchi, K. Nakatsugawa, J. Organomet. Chem. 94 (1975) 449.
[63] Y. Ito, T. Hirao, T. Saegusa, J. Org. Chem. 43 (1978) 1011.
[64] Y. Shvo, D. Czarkie, Y. Rahamim, D.F. Chodosh, J. Am. Chem. Soc. 108 (1986) 7400.
[65] Y. Blum, D. Czarkie, Y. Rahamim, Y. Shvo, Organometallics 4 (1985) 1459.
[66] C.P. Casey, S.W. Singer, D.R. Powell, R.K. Hayashi, M. Kavana, J. Am. Chem. Soc. 123 (2001) 1090.
[67] C.P. Casey, H. Guan, J. Am. Chem. Soc. 129 (2007) 5816.
[68] R. Noyori, T. Okhuma, Angew. Chem., Int. Ed. 40 (2001) 40.
[69] K.-J. Haack, S. Hashiguchi, A. Fujii, T. Ikariya, R. Noyori, Angew. Chem., Int. Ed. Engl. 36 (1997) 285.
[70] K. Abdur-Rashid, S.E. Clapham, A. Hadzovic, J.N. Harvey, A.J. Lough, R.H. Morris, J. Am. Chem. Soc. 124 (2002) 15104.
[71] K. Abdur-Rashid, A.J. Lough, R.H. Morris, Organometallics 19 (2000) 2655.
[72] K. Abdur-Rashid, M. Faatz, A.J. Lough, R.H. Morris, J. Am. Chem. Soc. 123 (2001) 7473.
[73] C.A. Sandoval, T. Ohkuma, K. Muniz, R. Noyori, J. Am. Chem. Soc. 125 (2003) 13490.
[74] R. Noyori, M. Koizumi, D. Ishii, T. Ohkuma, Pure Appl. Chem. 73 (2001) 227.
[75] T. Ohkuma, H. Ooka, S. Hashiguchi, T. Ikariya, R. Noyori, J. Am. Chem. Soc. 117 (1995) 2675.
[76] M. Yamakawa, H. Ito, R. Noyori, J. Am. Chem. Soc. 122 (2000) 1466.
[77] F. Hutschka, A. Dedieu, M. Eichberger, R. Fornika, W. Leitner, J. Am. Chem. Soc. 119 (1997) 4432.
[78] F. Hutschka, A. Dedieu, J. Chem. Soc., Dalton Trans. (1997) 1899.
[79] C.A. Mebi, B.J. Frost, Organometallics 24 (2005) 2339.
[80] M. Frey, Chem. Bio. Chem. 3 (2002) 153.
[81] J.P. Collman, Nat. Struct. Biol. 3 (1996) 213.
[82] P.E.M. Siegbahn, Adv. Inorg. Chem. 56 (2004) 101.
[83] M.Y. Darensbourg, E.J. Lyon, J.J. Smee, Coord. Chem. Rev. 206/207 (2000) 533.
[84] M.Y. Darensbourg, E.J. Lyon, X. Zhao, I.P. Georgakaki, Proc. Natl. Acad. Sci. U.S.A. 100 (2003) 3683.
[85] I.P. Georgakaki, M.Y. Darensbourg, Compr. Coord. Chem. II 8 (2004) 549.
[86] R.C. Linck, T.B. Rauchfuss, in: G. Jaouen (Ed.), Bioorganometallics: Biomolecules, Labeling, Medicine, Wiley–VCH Verlag GmbH & Co, KGaA, Weinheim, 2006, p. 403.
[87] Z. Chen, B.J. Lemon, S. Huang, D.J. Swartz, J.W. Peters, K.A. Bagley, Biochemistry 41 (2002) 2036.
[88] Y. Nicolet, A.L. de Lacey, X. Vernede, V.M. Fernandez, E.C. Hatchikian, J.C. Fontecilla-Camps, J. Am. Chem. Soc. 123 (2001) 1596.
[89] D. Sellmann, G.H. Rackelmann, F.W. Heinemann, Chem. Eur. J. 3 (1997) 2071.
[90] X. Zhao, I.P. Georgakaki, M.L. Miller, R. Mejia-Rodriguez, C.-Y. Chiang, M.Y. Darensbourg, Inorg. Chem. 41 (2002) 3917.
[91] J.W. Peters, W.N. Lanzilotta, B.J. Lemon, L.C. Seefeldt, Science 283 (1999) 35.
[92] A.L. De Lacey, V.M. Fernandez, M. Rousset, C. Cavazza, E.C. Hatchikian, J. Biol. Inorg. Chem. 8 (2003) 129.
[93] B.J. Lemon, J.W. Peters, Biochemistry 38 (1999) 12969.
[94] A. Farkas, L. Farkas, J. Yudkin, Proc. Roy. Soc. (Lond.) B 115 (1934) 373.
[95] B.K. Burgess, S. Wherland, W.E. Newton, E.I. Stiefel, Biochemistry 20 (1981) 5140.
[96] H.D. Hoberman, D. Rittenberg, J. Biol. Chem. 147 (1943) 211.
[97] R.H. Crabtree, Inorg. Chim. Acta 125 (1986) L7.
[98] R.T. Hembre, S. McQueen, J. Am. Chem. Soc. 116 (1994) 2141.
[99] P.M. Vignais, Coord. Chem. Rev. 249 (2005) 1677.
[100] L. Dahlenburg, R. Gotz, Eur. J. Inorg. Chem. (2004) 888.
[101] C. Bianchini, K. Linn, D. Masi, M. Peruzzini, A. Polo, A. Vacca, F. Zanobini, Inorg. Chem. 32 (1993) 2366.
[102] E.P. Cappellani, S.D. Drouin, G. Jia, P.A. Maltby, R.H. Morris, C.T. Schweitzer, J. Am. Chem. Soc. 116 (1994) 3375.
[103] B. Chin, A.J. Lough, R.H. Morris, C.T. Schweitzer, C. D'Agostino, Inorg. Chem. 33 (1994) 6278.
[104] V.I. Bakhmutov, Eur. J. Inorg. Chem. (2005) 245.
[105] J.C. Lee Jr., E. Peris, A.L. Rheingold, R.H. Crabtree, J. Am. Chem. Soc. 116 (1994) 11014.
[106] A.J. Lough, S. Park, R. Ramachandran, R.H. Morris, J. Am. Chem. Soc. 116 (1994) 8356.
[107] R.H. Crabtree, O. Eisenstein, G. Sini, E. Peris, J. Organomet. Chem. 567 (1998) 7.
[108] L.M. Epstein, E.S. Shubina, Coord. Chem. Rev. 231 (2002) 165.
[109] N.V. Belkova, E.S. Shubina, L.M. Epstein, Acc. Chem. Res. 38 (2005) 624.
[110] L.M. Epstein, N.V. Belkova, E.S. Shubina, in: M. Peruzzini, R. Poli (Eds.), Recent Advances in Hydride Chemistry, Elsevier, Amsterdam, 2001, p. 391.
[111] R. Custelcean, J.E. Jackson, Chem. Rev. 101 (2001) 1963.
[112] J.A. Ayllon, C. Gervaux, S. Sabo-Etienne, B. Chaudret, Organometallics 16 (1997) 2000.
[113] V.I. Bakhmutov, E.V. Bakhmutova, N.V. Belkova, C. Bianchini, L.M. Epstein, D. Masi, M. Peruzzini, E.S. Shubina, E.V. Vorontsov, F. Zanobini, Can. J. Chem. 79 (2001) 479.
[114] E.I. Gutsul, N.V. Belkova, M.S. Sverdlov, L.M. Epstein, E.S. Shubina, V.I. Bakhmutov, T.N. Gribanova, R.M. Minyaev, C. Bianchini, M. Peruzzini, F. Zanobini, Chem. Eur. J. 9 (2003) 2219.
[115] A. Dedieu, F. Hutschka, A. Milet, ACS Symp. Ser. 721 (1999) 100.
[116] A. Macchioni, Chem. Rev. 105 (2005) 2039.
[117] E.I. Gutsul, N.V. Belkova, G.M. Babakhina, L.M. Epstein, E.S. Shubina, C. Bianchini, M. Peruzzini, F. Zanobini, Russ. Chem. Bull. 52 (2003) 1204.
[118] L.S. Van der Sluys, J. Eckert, O. Eisenstein, J.H. Hall, J.C. Huffman, S.A. Jackson, T.F. Koetzle, G.J. Kubas, P.J. Vergamini, K.G. Caulton, J. Am. Chem. Soc. 112 (1990) 4831.
[119] A. Albinati, V.I. Bakhmutov, K.G. Caulton, E. Clot, J. Eckert, O. Eisenstein, D.G. Gusev, V.V. Grushin, B.E. Hauger, et al., J. Am. Chem. Soc. 115 (1993) 7300.
[120] P. Barrio, M.A. Esteruelas, A. Lledos, E. Onate, J. Tomas, Organometallics 23 (2004) 3008.
[121] D.G. Gusev, J. Am. Chem. Soc. 126 (2004) 14249.
[122] C.E. Webster, C.L. Gross, D.M. Young, G.S. Girolami, A.J. Schultz, M.B. Hall, J. Eckert, J. Am. Chem. Soc. 127 (2005) 15091.
[123] M. Schlaf, A.J. Lough, P.A. Maltby, R.H. Morris, Organometallics 15 (1996) 2270.

[124] M.G. Basallote, M. Besora, J. Duran, M.J. Fernandez-Trujillo, A. Lledos, M.A. Manez, F. Maseras, J. Am. Chem. Soc. 126 (2004) 2320.
[125] N.V. Belkova, M. Besora, L.M. Epstein, A. Lledos, F. Maseras, E.S. Shubina, J. Am. Chem. Soc. 125 (2003) 7715.
[126] N.V. Belkova, A.V. Ionidis, L.M. Epstein, E.S. Shubina, S. Gruendemann, N.S. Golubev, H.-H. Limbach, Eur. J. Inorg. Chem. (2001) 1753.
[127] T.P. Fong, C.E. Forde, A.J. Lough, R.H. Morris, P. Rigo, E. Rocchini, T. Stephan, J. Chem. Soc., Dalton Trans. (1999) 4475.
[128] M.G. Basallote, M. Besora, C.E. Castillo, M.J. Fernandez-Trujillo, A. Lledos, F. Maseras, M.A. Manez, J. Am. Chem. Soc. 129 (2007) 6608.
[129] G. Orlova, S. Scheiner, J. Phys. Chem. A 102 (1998) 260.
[130] G. Orlova, S. Scheiner, J. Phys. Chem. A 102 (1998) 4813.
[131] A. Rossin, L. Gonsalvi, A.D. Phillips, O. Maresca, A. Lledos, M. Peruzzini, Organometallics 26 (2007) 3289.
[132] D. Braga, P. De Leonardis, F. Grepioni, E. Tedesco, Inorg. Chim. Acta 273 (1998) 116.
[133] F. Maseras, A. Lledos, E. Clot, O. Eisenstein, Chem. Rev. 100 (2000) 601.
[134] P.A. Maltby, M. Schlaf, M. Steinbeck, A.J. Lough, R.H. Morris, W.T. Klooster, T.F. Koetzle, R.C. Srivastava, J. Am. Chem. Soc. 118 (1996) 5396.
[135] D.M. Heinekey, T.A. Luther, Inorg. Chem. 35 (1996) 4396.
[136] J.K. Law, H. Mellows, D.M. Heinekey, J. Am. Chem. Soc. 124 (2002) 1024.
[137] S. Gruendemann, H.-H. Limbach, G. Buntkowsky, S. Sabo-Etienne, B. Chaudret, J. Phys. Chem. A 103 (1999) 4752.
[138] N.S. Hush, J. Am. Chem. Soc. 119 (1997) 1717.
[139] R. Gelabert, M. Moreno, J.M. Lluch, A. Lledos, V. Pons, D.M. Heinekey, J. Am. Chem. Soc. 126 (2004) 8813.
[140] R.H. Crabtree, M. Lavin, J. Chem. Soc., Chem. Commun. (1985) 1661.
[141] V.I. Bakhmutov, Practical NMR Relaxation for Chemists, John Wiley & Sons, Ltd., West Sussex, 2004.
[142] P.J. Desrosiers, L. Cai, Z. Lin, R. Richards, J. Halpern, J. Am. Chem. Soc. 113 (1991) 4173.
[143] K.A. Earl, G. Jia, P.A. Maltby, R.H. Morris, J. Am. Chem. Soc. 113 (1991) 3027.
[144] M.T. Bautista, K.A. Earl, P.A. Maltby, R.H. Morris, J. Am. Chem. Soc. 110 (1988) 4056.
[145] V.I. Bakhmutov, in: M. Peruzzini, R. Poli (Eds.), Recent Advances in Hydride Chemistry, Elsevier, Amsterdam, 2001, p. 375.
[146] V.I. Bakhmutov, C. Bianchini, F. Maseras, A. Lledos, M. Peruzzini, E.V. Vorontsov, Chem. Eur. J. 5 (1999) 3318.
[147] V.I. Bakhmutov, Magn. Reson. Chem. 42 (2004) 66.